
Health and Kinesiology Theses

Department of Health and Kinesiology

Fall 12-10-2019

Characterization of the Nuclear Pore Complex in Red Alga, Cyanidioschyzon merolae

Michelle Veronin
University of Texas at Tyler

Follow this and additional works at: https://scholarworks.uttyler.edu/hkdept_grad



Part of the Biochemistry Commons, Medicine and Health Sciences Commons, Molecular Biology Commons, and the Structural Biology Commons

Recommended Citation

Veronin, Michelle, "Characterization of the Nuclear Pore Complex in Red Alga, Cyanidioschyzon merolae" (2019). *Health and Kinesiology Theses*. Paper 16.
<http://hdl.handle.net/10950/2311>

This Thesis is brought to you for free and open access by the Department of Health and Kinesiology at Scholar Works at UT Tyler. It has been accepted for inclusion in Health and Kinesiology Theses by an authorized administrator of Scholar Works at UT Tyler. For more information, please contact tgullings@uttyler.edu.

CHARACTERIZATION OF THE NUCLEAR PORE COMPLEX IN RED
ALGA, CYANIDIOSCHYZON MEROLAE

by

MICHELLE VERONIN

A thesis submitted in partial fulfillment
of the requirements for the degree of
Master of Science in Health Sciences
Department of Health and Kinesiology
Cheryl Cooper, Ph.D., Committee Chair
College of Nursing and Health Sciences

The University of Texas at Tyler
December 2019

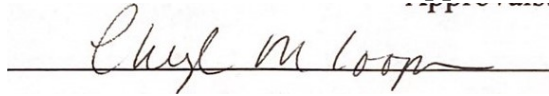
The University of Texas at Tyler
Tyler, Texas

This is to certify that the Master's Thesis of

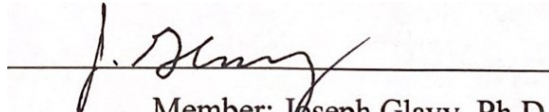
MICHELLE VERONIN

has been approved for the thesis requirement on
November 13, 2019
for the Master of Science in Health Sciences degree

Approvals:

A handwritten signature in cursive script, appearing to read "Cheryl M. Cooper", written over a horizontal line.

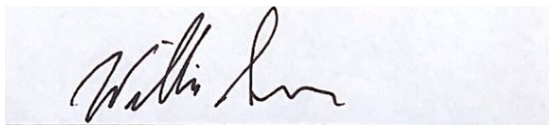
Thesis Chair: Cheryl Cooper, Ph. D.

A handwritten signature in cursive script, appearing to read "J. Glavy", written over a horizontal line.

Member: Joseph Glavy, Ph.D.

A handwritten signature in cursive script, appearing to read "Ayman", written over a horizontal line.

Member: Ayman Hamouda, Ph.D.

A handwritten signature in cursive script, appearing to read "William Sorensen", written over a horizontal line.

Member: William Sorensen, Ph.D.

Acknowledgements

I would like to thank the members of my thesis committee including my committee chair, Dr. Cheryl Cooper, and Dr. Joseph Glavy, Dr. Ayman Hamouda, and Dr. William Sorensen of the University of Texas at Tyler, for their guidance and support in the completion of this project.

I would also like to thank the members of the Glavy Lab at the Fisch College of Pharmacy, including Dr. Joseph Glavy and Benjamin Jordan for their advice and assistance in the research process, and Kevin Tokoph for his contribution to the designing of figures.

I would also like to thank the members of NYU Langone's Proteomics Laboratory at the NYU Langone Medical Center for their contribution of the proteomics data used for analysis of *C. merolae*, Dr. Beatrix Ueberheide and Joshua Andrade.

I would also like to thank the members of the Beck Lab at the European Molecular Biology Laboratory for their contribution of the SEM and TEM data used for structural analysis of *C. merolae*, Dr. Martin Beck and Christian Zimmerli.

I would also like to thank Thomas Cattabiani of Stevens Institute of Technology for his role in operational training on the confocal microscope.

Table of Contents

List of Tables	iii
List of Figures.....	iv-v
Abstract.....	vi
Chapter One: Introduction	1
Chapter Two: Review of the Literature.....	3
<i>Cyanidioschyzon merolae</i>	3
Nuclear Pore Complex.....	7
NPC Structure.....	8
Role of the NPC in Mitosis.....	9
Nucleoporins (Nups).....	10
NE and NPC-associated Disease States.....	18
Cancer.....	18
Huntington’s Disease.....	20
Premature and Accelerated Aging.....	21
Objectives.....	26
Chapter Three: Methods.....	27
Nuclear Extract Isolation Methods.....	27
Western Blotting.....	27
Chloroplast Removal and Nuclei Isolation.....	28
Proteomics.....	29
Immunofluorescence, Confocal Microscopy, and Live Cell Imaging.....	30
ER/Mitochondria Labeling.....	31
Electron Microscopy.....	32
Chapter Four: Results.....	34
Nuclear Isolation.....	34
Proteomics.....	38

Immunofluorescence and Confocal Microscopy.....	41
Electron Microscopy.....	41
Chapter Five: Discussion.....	47
References.....	52
Appendix A.....	66
Appendix B.....	67
Appendix C.....	68

List of Tables

Table 1: Antibodies tested by Western blotting that generated positive or negative reactions.....36

Table 2: Nups identified by proteomics in *C. merolae* nuclear extract.....40

List of Figures

Figure 1: Microscope image of <i>C. merolae</i> cells and constituents of <i>C. merolae</i> genome.....	3
Figure 2: Comparison between the NPCs of higher plants and vertebrates with a question mark for <i>C. merolae</i>	6
Figure 3: <i>C. merolae</i> nuclear extract gel transfer.....	34
Figure 4: Western blotting of antibodies against several Nups and MAb414 in <i>C. merolae</i> whole cell extract, cytoplasmic fractions 2 and 3, and nuclear extract.....	35
Figure 5: Flow chart illustrating each step of the fractionation process by which nuclei was isolated and samples collected at each step.....	37
Figure 6: Summary of gel digestion methods used for proteomic analysis of <i>C. merolae</i>	39
Figure 7: Summary of peptide extraction methods used for proteomic analysis of <i>C. merolae</i>	39
Figure 8: Nups identified by proteomics in <i>C. merolae</i> nuclear extract, categorized by major group and compared to known Nups in humans within each respective group.....	40
Figure 9: Immunofluorescent microscopy analyses of NE-associated proteins including Nup107 and NDC1 as well as the ER-associated protein KDEL in <i>C. merolae</i>	42
Figure 10: Confocal microscopy analyses <i>C. merolae</i> cells labeled with ER and mitochondria dyes.....	43
Figure 11: Live cell images of <i>C. merolae</i> at time points 26-28, each taken 1 minute apart.....	44
Figure 12: Scanning electron microscopy analyses of the external surface of <i>C. merolae</i> cells.....	45
Figure 13: Transmission electron microscopy analysis of <i>C. merolae</i>	46

Figure 14: Expected timeline to complete specific aims of
project.....50

Abstract

CHARACTERIZATION OF THE NUCLEAR PORE COMPLEX IN RED
ALGA, CYANIDIOSCHYZON MEROLAE

Michelle Veronin

Thesis chair: Cheryl Cooper, Ph.D.

The University of Texas at Tyler
December 2019

Cyanidioschyzon merolae (*C. merolae*) is a primitive, unicellular species of red alga that is considered to be one of the simplest self-sustaining eukaryotes. The highly elementary nature of *C. merolae* makes it an excellent model organism for studying evolution as well as cell function and organelle communication. *In our study, we hypothesize that C. merolae contains the minimal assembly of proteins to make up their Nuclear Pore Complexes (NPCs), and hence are the first ancestral NPCs.* NPCs are essential for basic nuclear transport in the cell. They are embedded in the double membrane of the nucleus, the nuclear envelope (NE), which separates nuclear DNA from cytoplasmic organelles. The NE acts as a selective protective barrier, and active transport of molecules between the nucleus and the cytoplasm is facilitated mainly by nuclear NPCs in higher and lower eukaryotic cells. When not functioning properly or fully, NPCs are known to be involved in several types of human disease, including cancer, accelerated aging and Huntington's Disease (HD).

Chapter One

Introduction

Cyanidioschyzon merolae (*C. merolae*) is a primitive, unicellular species of red alga that is considered to be one of the simplest self-sustaining eukaryotes. The highly elementary nature of *C. merolae* makes it an excellent model organism for studying evolution as well as cell function and organelle communication. Yeast (*Saccharomyces cerevisiae*) is a single-celled eukaryote that has been commonly utilized as a model system for studying biological processes and molecular structure, including the structure and function of the nuclear pore complex (NPC). However, there are differences between yeast and human cells, such as the type of mitosis, that create limitations associated with what can be applied to human biology from studies using this system. The ability to accurately study the NPC is critical, as NPCs are essential for basic nuclear transport in the cell. Nearly all molecular traffic that travels between the nucleus and cytoplasm is directed through NPCs. NPCs are composed of approximately 30 specialized proteins known as nucleoporins (Nups) that are present in highly repeated copies. Additionally, when their function is compromised, NPCs are involved in many human disease states.

Phylogenetic studies indicate that *C. merolae* diverged early in eukaryotic lineage, but its primitive features appear to have been conserved throughout evolution. The *C. merolae* genome is only 16.5 Mbp distributed over 20 chromosomes. Complete genomic sequencing revealed the presence of only 27 introns and approximately 5,331 protein-coding genes (Matsuzaki et al., 2004). Another advantage of studying *C. merolae* is its

very primitive internal organization. It has only one nucleus, one mitochondrion, and a minimal set of membrane-bound organelles: one peroxisome, one Golgi apparatus, and a small number of lysosomes. Organellar dynamics have been studied in *C. merolae*, and these findings have suggested that organelles behave as if they are linked (Gibbs, 1962a, 1962b; Misumi et al., 2005). (Yagisawa et al., 2012; Yagisawa et al., 2013). Therefore, it is an ideal candidate to resolve the design of organelle biogenesis and behavior during the cell cycle. In Plantae, the mechanism of mitosis (i.e., open or closed mitosis) remains unclear, which is why it is critical to study simple red algae like *C. merolae* at mitosis to fit the context of functionality and evolution (Ciska & Moreno Diaz de la Espina, 2014; Evans, Clark, Whipple, & Whitham, 2012; Graumann & Evans, 2011; Imoto, Yoshida, Yagisawa, Kuroiwa, & Kuroiwa, 2011; Meier, 2001; Misumi et al., 2005). Preliminary data indicates an open mitosis in *C. merolae*, the same mechanism observed in human cells.

It has been shown that vertebrates and plants share similar patterns of Nups (Neumann, Jeffares, & Poole, 2006; Tamura, Fukao, Iwamoto, Haraguchi, & Hara-Nishimura, 2010). Currently, analyses of *C. merolae*'s protein composition have been lacking, with initial homology matching failing to identify over half of typical Nups in its NPC. The purpose of the present investigation is to characterize the NPC of *C. merolae* through the incorporation of additional methods to build on preliminary evidence that has evaluated the *C. merolae* NPC protein composition. I hypothesize that *C. merolae* has the most basic protein assembly that makes up its NPC, and thus possess the most ancestral eukaryotic NPCs.

Chapter Two

Review of the Literature

Cyanidioschyzon merolae

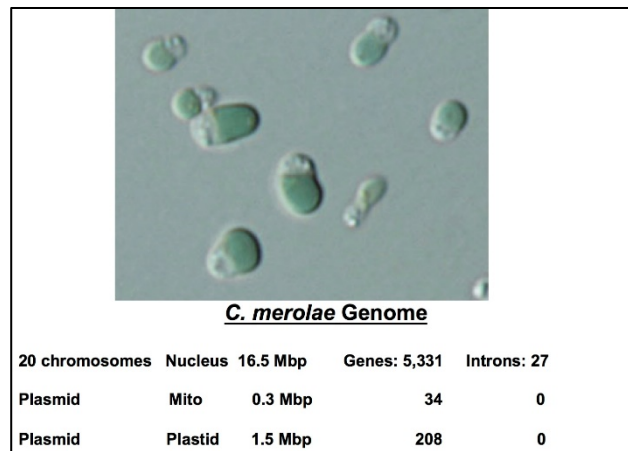


Figure 1.

Microscope image of *C. merolae* cells and constituents of *C. merolae* genome.

C. merolae is a primitive, unicellular species of red alga that was originally isolated from hot springs in Naples, Italy. The typical habitat of *C. merolae* is sulfate-rich, acidic environments; it can withstand temperatures of 45°C and a pH below 2 (Misumi et al., 2005). It is a small (μm), club-shaped red alga that does not actually appear red. This thermophilic organism is considered to be one of the simplest eukaryotes. It has no cell wall, as although the genes encoding proteins of the cell wall are present, they are not

expressed. Organellar dynamics have been studied in *C. merolae*, including inheritance of the Golgi body and endoplasmic reticulum (ER) (Yagisawa et al., 2012; Yagisawa et al., 2013). The running hypothesis is that organelles behave as if they are linked (Gibbs, 1962a, 1962b; Misumi et al., 2005). Therefore, it is an ideal candidate to resolve the design of organelle biogenesis and behavior during the cell cycle.

Optimal growth conditions for *C. merolae* cells are 42°C in MA2 media at pH 2.7 (Imoto et al., 2010; Imoto et al., 2011; Misumi et al., 2005). Cells can grow slowly with a CO₂ level between 1-2% with gentle shaking or more rapidly with 5% CO₂ bubbling (Imoto et al., 2011). In order to study the cell cycle, reliable cell synchronization is necessary. *C. merolae* provides this by two different methods. Its cell cycle phase can be easily synchronized by light and dark cycles. Specifically, by strategic triggering of photosynthesis in conjunction with altering CO₂ levels, cells can be coordinated and isolated in different phases of the cell cycle (Fujiwara, Tanaka, Kuroiwa, & Hirano, 2013; Imoto et al., 2011). Cells can also be synchronized by drug treatment with microtubule binding drugs such as oryzalin (Fujiwara et al., 2013). With these options, *C. merolae* is an ideal system to study mitotic changes, but targets are lacking or yet to be discovered.

One study provided a comprehensive analysis of two structures involved in mitosis, condensins I and II, in *C. merolae* (Fujiwara et al., 2013). Condensins are protein complexes that have important functions in chromosome condensation and segregation during mitosis and meiosis (Cuylen & Haering, 2011; Fujiwara et al., 2013; Hirano, 2012). While the corresponding subunits specific to condensin II have not previously been found in fungi, both condensins were described in *C. merolae* and were revealed to have notable

similarity to vertebrate condensins in terms of dynamics and localization (Fujiwara et al., 2013).

Characterization of endoplasmic reticulum (ER) inheritance suggests that *C. merolae* possesses a nuclear ER as well as a smaller amount of peripheral ER that extends from the nuclear ER (Yagisawa et al., 2012). It appears that the nuclear ER undergoes division during mitosis, while the peripheral ER formed ring-like structures during G1 and S phases and extended toward the mitochondria and cell division planes during M phase, implying a closed mitosis in *C. merolae* (Yagisawa et al., 2012). However, investigation into cell cycle dynamics involving condensins revealed evidence supporting more of an open mitosis mechanism. Using immunofluorescence markers, partial dissolving of the NE was observed as well as dispersion of the NPCs in the cytoplasm during metaphase (Fujiwara et al., 2013). Specifically, these findings indicated that the means by which condensin I accesses chromosomes is through the partially dissolved NEs (Fujiwara et al., 2013).

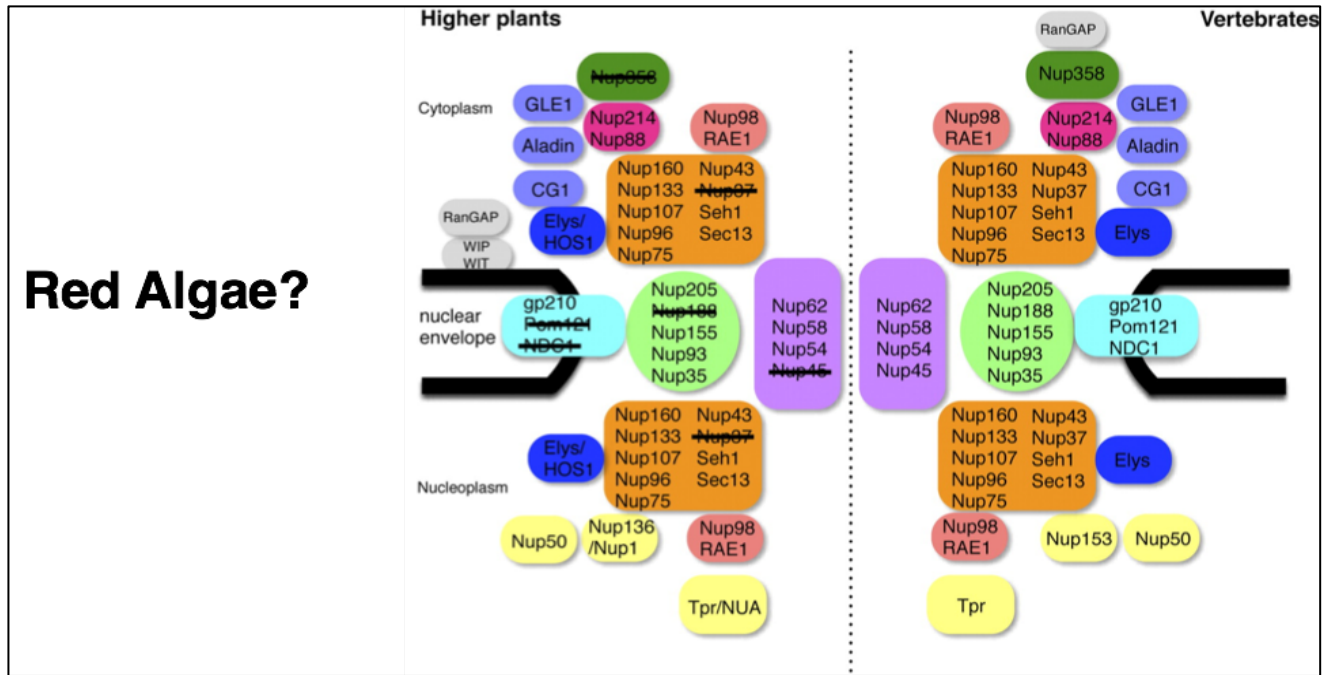


Figure 2.

Comparison between the NPCs of higher plants and vertebrates with a question mark for *C. merolae*.

A full set of genetic tools has been developed and tested successfully in *C. merolae*. The establishment of a transient gene expression system in *C. merolae*, which has allowed for expression of exogenous DNA, indicates its utility for molecular genetic analyses (Ohnuma, Yokoyama, Inouye, Sekine, & Tanaka, 2008). Additionally, the GFP reporter system has been applied in *C. merolae* in order to investigate the subcellular localization of proteins (Watanabe, Ohnuma, Sato, Yoshikawa, & Tanaka, 2011). A method of gene suppression has also been effectively established in *C. merolae*. Ohnuma and colleagues transformed *C. merolae* cells with antisense DNA of the catalase gene and subsequently observed reduced catalase expression (Ohnuma et al., 2009).

Nup arrangements in vertebrates and plants are remarkably similar (Neumann et al., 2006; Tamura et al., 2010). *Arabidopsis thaliana* is missing just six Nups when compared to vertebrates. Additionally, it was shown to contain unique Nups like Nup136. Despite these differences, both proceed with an open mitosis. Questions have arisen with regard to the Nups and pore membrane (POM) proteins that compose the *C. merolae* NPC (Neumann et al., 2006). Initial homology matching has met with only limited success. More than half of typical Nups are missing in the NPC of *C. merolae*. This may represent the primitive NPC and/or a collection of novel *C. merolae* Nups yet to be discovered.

Nuclear Pore Complex

A distinguishing feature of eukaryotic cells from prokaryotic cells is the separation of nuclear DNA from cytoplasmic organelles. This separation is in the form of the nuclear envelope (NE), a structure that is considered to be a specialized endoplasmic reticulum (ER) membrane containing a double bilayer that has an inner and outer membrane system. Such segregation is necessary for the proper organization of nuclear import and export of materials required for basic cellular processes, including transcription factors, RNAs, kinases, and viral particles (Tran & Went, 2006; Weis, 2003). Nuclear pore complexes (NPCs) are large protein complexes situated in circular openings flanked by a fusion of the outer and inner nuclear membrane (Kabachinski & Schwartz, 2015; Tran & Went, 2006; Weis, 2003). NPCs essentially act as gateways through which macromolecular traffic is directed into and out of the nucleus, a process that is mediated by highly regulated pathways. NPCs facilitate nearly all transport that occurs between the nucleus and cytoplasm (Kabachinski & Schwartz, 2015). Overall, the process of nucleocytoplasmic transport occurs sequentially by the binding of molecules to transport receptors, passage

through the NPC, and translocation from the NPC to intranuclear or cytoplasmic target sites (Hoelz & Blobel, 2004; Lim, Aebi, & Fahrenkrog, 2008).

NPCs are composed of approximately 30 different specialized proteins, known collectively as nucleoporins (Nups) that are highly repeated (Rout et al., 2000; Rout & Wente, 1994; Schwartz, 2005). Nups have been associated with numerous human diseases, including various forms of cancer, viral infection, and Huntington's Disease (HD).

NPC Structure

The NPC is a large macromolecular assembly with an estimated size of 110 MDa in vertebrates and 60 MDa yeast (Bui et al., 2013; Hoelz, Glavy, & Beck, 2016; Kosinski et al., 2016; von Appen et al., 2015). NPCs possess a symmetric core with an octahedral arrangement across the double membrane of the NE, resembling the spokes of a bicycle wheel. Nups of the NPC have been categorized through proteomic studies in yeast and metazoa (Cronshaw, Krutchinsky, Zhang, Chait, & Matunis, 2002; Rout et al., 2000). It has been shown that mammalian NPCs contain at least seven additional Nups including ALADIN, Nup358, POM210, POM121, NDC1, Nup43, and Nup37. Nups can be classified into six categories: (1) Y-complex (coat) Nups, (2) Adaptor Nups, (3) Channel Nups, (4) Cytoplasmic filament Nups, (5) nuclear basket Nups (6) POM (transmembrane) Nups. Nups are typically named by their designated molecular weight and are organized into macromolecular assemblies called subcomplexes. In the laboratory, interphase subcomplexes can be isolated through biochemical extraction of the NE with low percentage non-ionic or zwitterionic detergent treatment. (Belgareh et al., 2001; Glavy et al., 2007; Walther et al., 2003). A key feature of NPCs is that these modular units are present in multiple copies arranged around two- and eightfold axes of symmetry, and

discrete structures are formed within the NPC (Schwartz, 2005). Overall NPC architecture is conserved between yeast and higher eukaryotes with an eightfold symmetry (Aaronson & Blobel, 1974; Schwartz, 2005)

Cryo-electron tomography with three-dimensional reconstruction gives a resolution of 23 Angstroms (Bui et al., 2013; Kosinski et al., 2016). The nuclear basket extends nearly 60 nm into the nucleus (Beck et al., 2004; Beck, Lucic, Forster, Baumeister, & Medalia, 2007; Bonny, Hull, & Howell, 2014; Bui et al., 2013). The central core inner ring (IR) is estimated at less than 50 nm while the envelope is approximately 50 nm (Beck et al., 2007). The cytoplasmic rings (CRs) are believed to act as a docking site for protein transport and bind to nuclear rings (NRs) (Beck et al., 2004; Beck et al., 2007; Bui et al., 2013; Kosinski et al., 2016; von Appen et al., 2015). An early approach using a combination of proteomic data with a computational platform has been applied to the architectures of the macromolecular assemblies of the NPC (Alber et al., 2007). This study concluded that the fundamental symmetry unit of the NPC is the spoke (Alber et al., 2007). Within the ringed structure are linked units and flexible repeat units that both stabilize and are involved in transport (Tran & Wentz, 2006). The inner and outer rings help to facilitate the membrane structure. The complete architecture of the NPC includes some non-Nup proteins: the nuclear membrane proteins and the nuclear lamina (Schwartz, 2005). These non-Nup proteins make up the surrounding regions of the NPC and support its transport function.

Role of the NPC in Mitosis

In human dividing cells, NPCs undergo a cycle of disassembly and assembly in concert with the cell cycle. In this form of open mitosis, the NE completely dissipates during mitosis, which opens up the nucleus and exposes the chromosomes to the cytoplasm.

The NE breaks down early in mitosis as the chromosomes become condensed, allowing microtubules that originate from microtubule organizing center (MTOC) to attach with the chromosomes via kinetochores. Nup subcomplexes release from the NPC during open mitosis and are the disassembly units of the NPC (Hetzer, Walther, & Mattaj, 2005). During mitosis, chromosomes align to the metaphase plate, followed by separation of sister chromatids at anaphase. The NE begins to reassemble, shortly afterward, in telophase. Once the NE is completely assembled, the nucleus expands and the chromosomes decondense to interphase. In closed mitosis, the NE persists throughout the cell cycle, preventing “opening” of the nucleus to the cytoplasm.

During closed mitosis, the spindle-pole bodies nucleate microtubules within the nucleus and the processes occur within the encapsulated mitotic NE (Boettcher & Barral, 2013; Jaspersen & Ghosh, 2012; Webster, Witkin, & Cohen-Fix, 2009; D. Zhang & Oliferenko, 2013). A variation of both has been observed in some species, called semi-open, exhibiting a partial breakdown of the NE. There exists a clearly defined difference between vertebrates (open mitosis) and yeast (closed mitosis). Closed mitosis may reflect the most ancient mechanism of eukaryotic cell division, whereas open mitosis appears to have been conceived and re-conceived during evolution (Boettcher & Barral, 2013).

Nucleoporins (Nups)

Y-Nups

Y-Nups are contained within the Y-complex of the NPC, also known as the Nup107 subcomplex. The cytoplasmic Y-complex has nine members: Nup160, Nup133, Nup107, Nup96, Nup75, Nup43, Nup37, Seh1, and Sec13 while the nuclear Nup107 subcomplex

contains a tenth member: ELYS (Bui et al., 2013; Cristea, Williams, Chait, & Rout, 2005; Fontoura, Blobel, & Matunis, 1999; Glavy et al., 2007; Loiodice et al., 2004; Ori et al., 2013; von Appen et al., 2015). This subcomplex has been classified as a keystone of NPC assembly (Boehmer, Enninga, Dales, Blobel, & Zhong, 2003). RNAi knockdown experiments of individual members within the Y-complex affect select members of the subcomplex in addition to some other Channel Nups (Boehmer et al., 2003; Walther et al., 2003). These findings show the interdependence of subcomplex members and the overall NPC. Positioned at the curvatures of the membrane embedding the NPC, the Y-complex acts to stabilize these bends in the membrane (Boehmer, Jeudy, Berke, & Schwartz, 2008).

Early reconstitution experiments in yeast produced a Y-complex, which was visualized through negative staining electron microscopy (Lutzmann, Kunze, Buerer, Aebi, & Hurt, 2002). It was shown that the structural modules of the subcomplex are a collection of alpha-helical repeats and β -propellers. Through X-ray crystallography, the NPC can be gradually pieced together with the Y-complex as the main component. Larger crystal approaches have yielded great progress. A yeast hexameric Y-complex was achieved using a single domain synthetic antibody crystallization chaperone (Stuwe et al., 2015). Among the information provided was further proof of an evolutionarily conserved ring structure formed by the yeast Y-complex. Cryo-electron topography work has shown that the human Y-complex forms two reticulated rings on the cytoplasmic and the nuclear side (Hoelz et al., 2016; Kosinski et al., 2016; von Appen et al., 2015). Numerous discrete crystal structures of the Y-complex fit directly into the tomographic map including the yeast hexameric structure (Bui et al., 2013; Hoelz et al., 2016; Kosinski et al., 2016; von Appen et al., 2015). In an integrated approach coupling electron tomography, single-particle

electron microscopy, and crosslinking mass spectrometry, it was shown that 32 copies of the Y-complex amass into two reticulated rings, one at each of the cytoplasmic and nuclear face of the NPC (Bui et al., 2013). This twin-ring organization of the Y-complex explains the structural plasticity of the NPC (Bui et al., 2013). Flexible and spring-shaped hinges confer large-scale rearrangements that might be relevant for large unit transport (Bui et al., 2013).

Adaptor Nups

The Adaptor complex includes five members: Nup93, Nup205, Nup188, Nup155, and Nup35 (Hawryluk-Gara, Shibuya, & Wozniak, 2005). The X-ray crystal structure of Nup93 reveals an elongated, alpha-helical structure (Jeudy & Schwartz, 2007). This form is evolutionarily conserved and therefore functionally maintained (Jeudy & Schwartz, 2007). Members of the Adaptor complex contain mainly alpha-helical domains (Jeudy & Schwartz, 2007). Just like the Y-complex, Nup93 is a highly abundant protein with 32 copies within the NPC (Ori et al., 2013). The Nup93 subcomplex aids in inner ring stabilization and is needed for correct nuclear pore assembly and homeostasis of the NPC (Jeudy & Schwartz, 2007). RNAi experiments suggest a functional link between NE transmembrane NDC1, Nup93, and Nup205, as well as an anchor point function for the Nup93 subcomplex (Antonin, Ellenberg, & Dultz, 2008). This has been confirmed by structure studies showing that Nup93 is a key component to the IR. Furthermore, Nup62, a Channel Nup, has been shown to interact with Nup93, illustrating interdependence between IR Nups and the Channel Nups (Antonin et al., 2008). It has been demonstrated that 32 copies of both Nup188 and Nup205, Nup93, Nup155, and the Channel Nups fit into the IR with additional Nup155 protein reaching up to connect to the outer ring. The IRs

comprise rings similar to the Y-complex, confirming their evolutionary connection (Kosinski et al., 2016).

Channel Nups

Channel Nups have stretches of FG (Phe-Gly) repetitive residues which are separated by polar spacer regions of variable lengths (Lim et al., 2008; Tran & Wentz, 2006). FG repeat domains arrange into unstructured regions that form weak interactions with transporting proteins called karyopherins (kaps) (Tran & Wentz, 2006). Channel Nups like the Nup62 subcomplex are located in the inner pore region or central core inner ring (IR) (Beck et al., 2004; Beck et al., 2007). The Nup62 subcomplex includes Nup62, Nup58-Nup45, and Nup54 (Melcak, Hoelz, & Blobel, 2007; Schwartz, 2005). This subcomplex has been referred to as the central plug region of the NPC. While these transport Nups line the inner NPC, it is unlikely that they form a plug against transport, but rather a dynamic transport area of the complex. The FG repeat domains form tentacle-like structures that emanate from and line the channel of the pore. Additionally, they are shown to line the IR region.

Cytoplasmic Filament Nups

As in the case of Channel Nups, Cytoplasmic Filament Nups possess FG regions. Their floppy tentacle nature is cohesive with crystal formation. Thus far, only non-FG regions of these Nups have been reported. The X-ray crystal structure of the non-FG repeat N-terminus of Nup214 reveals a seven-bladed β -propeller with a segment of its C-terminus bound to the propeller (Napetschnig, Blobel, & Hoelz, 2007). Furthermore, X-ray analysis of Nup58-45 revealed a possible circumferential sliding mechanism to adjust the diameter

of the central transport channel (Melcak et al., 2007). The alpha-helical region forms a distinct tetramer with a hydrophobic interface. The residues are laterally displaced in numerous tetramer conformations giving the possibility of a sliding structure (Melcak et al., 2007). Selective knockdown of Nup214 followed by Cryo-ET demonstrates that this subcomplex protrudes into the cytoplasmic ring region (Bui et al., 2013). This position secures FG repeats onto the framework of the rings to facilitate nuclear transport (Bui et al., 2013). Further application of gene-silencing/Cryo-ET uncovered a role for Nup358 to stabilize solely the cytoplasmic reticulated double ring structure (von Appen et al., 2015). These findings change the edges between Y and Cytoplasmic filament Nups (von Appen et al., 2015).

Nuclear Basket Nups

Nup153, Nup50, and TPR (Translocated promoter region protein) comprise the nuclear basket and provide the surface to utilize binding areas for transport. TPR is an unusual Nup with more filament protein properties than most yet required for trafficking across the nuclear envelope. TPR acts as a framework component in the nuclear segment and tethers chromatin to begin perinuclear heterochromatin exclusion zones. Additionally, TPR is believed to act as a docking site for expressing genes interacting with select Nups. It participates in both nuclear import and export pathways for proteins with or without NES as well as the export of mRNA (Rajanala & Nandicoori, 2012; Rajanala et al., 2014). TPR coiled-coiled domains help give reliable support to form and maintain the nuclear basket. TPR also plays a role in mitotic spindle checkpoint signaling (Rajanala & Nandicoori, 2012; Rajanala et al., 2014). Within the nuclear basket, Nup153 is associated with TPR and contains four zinc fingers, which increase the local Ran concentration to assist nuclear

transport. Along with Nup50, Nup153 helps to terminate karyopherin-mediated transport (Tran & Wente, 2006).

POM Nups

The NE is separated into three domains: the outer nuclear membrane (ONM), the pore membrane (POM) and the inner nuclear membrane (INM) (Lusk, Blobel, & King, 2007). The POM region is the sector of the NE where INM and ONM fusion occurs. The POM curvatures are lined with select membrane proteins believed to anchor NPCs, similar to the settings of a ring. POM proteins are involved in the initiation of pore complex formation, stabilization, release, and reformation of the NPC. To date, four POM proteins: gp210, POM121, NDC1, and POM33 have been classified through proteomic and genetic screenings. The largest POM protein, gp210, also known as POM210, contains a single transmembrane domain as do the rest of the POM proteins. NDC1 is found both in the POM region and the spindle pole body (SPB) during mitosis. In yeast, it functions at the SPB and helps to anchor the SPB at the NE. However, in human cells, its purpose is still unknown (Kupke, Malsam, & Schiebel, 2017). Through RNAi experiments, a connection between the NE membrane, NDC1, and members of the adaptor complex, Nup93 and Nup205, was revealed, suggesting that the Nup93 subcomplex functions as an anchor point (Antonin et al., 2008; Mansfeld et al., 2006). Lack of NPC assembly and resulting formation of continuous nuclear membranes has been observed upon removal of POM121 (Antonin & Mattaj, 2005). There is no single POM or combination of POMs that is completely indispensable for survival, which implies structural or functional redundancy. However, upon removal of NDC1 and POM121, it was observed that these cells experienced the greatest disturbance in nuclear import and soluble Nup localization (Chen,

Smoyer, Slaughter, Unruh, & Jaspersen, 2014; Mansfeld et al., 2006; Mitchell, Mansfeld, Capitanio, Kutay, & Wozniak, 2010).

NDC1 was shown to form a linkage between the NE and soluble Nups and depletion of NDC1 shows markedly reduced Channel Nup staining compared to NDC1/control siRNA treatment (Mansfeld et al., 2006; Onischenko, Stanton, Madrid, Kieselbach, & Weis, 2009; Stavru et al., 2006). These results suggest a crucial role for NDC1 in structure, function, Nuclear Envelope Breakdown (NEBD) and assembly. POM protein “put back” experiments fail to restore function, implying the need for additional components as well as POM proteins (Franz et al., 2005; Mansfeld et al., 2006; Stavru et al., 2006). POM121 has demonstrated localization with Nups at forming nuclear pores (Doucet & Hetzer, 2010). In fact, a fragment of POM121 has a dominant-negative effect on pore assembly, suggesting a critical role of POM121 in assembly and nuclear pore biogenesis (Shaulov, Gruber, Cohen, & Harel, 2011). Specifically, the protein’s repeat-containing POM domain is involved in anchoring components of the pore complex to the pore membrane, as indicated by the formation of cytoplasmic annulate lamellae and when overexpressed in cells (Funakoshi, Clever, Watanabe, & Imamoto, 2011; Funakoshi et al., 2007). Interactions of POM121 with Nup155 and Nup160 are foreseen to contribute to the formation of the nuclear pore as well as the fastening of the NPC to the pore membrane (Mitchell et al., 2010). The newest POM protein, POM33, is required for proper NPC distribution (Chadrin et al., 2010; Floch et al., 2015) as well as assembly. However, a percentage of POM33 resides in the endoplasmic reticulum (ER) (Chadrin et al., 2010; Floch et al., 2015). It has been shown that gp210 is important for effective NPC disassembly, which suggests that phosphorylation of gp210 is an early event in NEBD

(Galy et al., 2008). Yet, the role of this set of POM proteins at the onset of disassembly is undetermined.

Mobile Nup: Nup98

Nup98 is found both at the NPC and within the nucleus, and it has multiple functions and binding partners (Fontoura et al., 1999; Tamura et al., 2010). Nup98 arises from a Nup98-Nup96 precursor form that splits by a self-cleavage domain similar to those found in *Drosophila* Hedgehog and *Flavobacterium* glycosylasparaginase (Fontoura et al., 1999; Rosenblum & Blobel, 1999). It is classified as a non-subcomplex or mobile Nup with multiple locations along both sides of the NPC (Fontoura et al., 1999). The function of Nup98 encompasses roles in transport, mitotic progression, gene expression, epigenetic changes and viral infection (Chakraborty et al., 2009; Chakraborty et al., 2008; Franks et al., 2017; Liang, Franks, Marchetto, Gage, & Hetzer, 2013; Mor, White, & Fontoura, 2014; Tamura et al., 2010). Part of the mitotic function of Nup98 includes a role in nuclear envelope breakdown (NEBD) (Laurell et al., 2011; Linder et al., 2017). Specifically, mitotic Phospho-Nup98 is a determining factor in NPC disassembly (Laurell et al., 2011; Laurell & Kutay, 2011). Additionally, one of Nup98's interacting partners is Rae1; together they act as temporal regulators of the anaphase-promoting complex (Jeganathan, Malureanu, & van Deursen, 2005).

Nup98 has also been linked to viral infection. In the case of influenza, down-regulation of Nup98 by the virus non-structural protein 1 (NS1) correlates with increased viral replication (Mor et al., 2014; Satterly et al., 2007). It has also been shown the Nup98 is targeted for degradation in cells infected with poliovirus, which is likely facilitated by a viral 2A protease. Poliovirus additionally targets two other Nups, Nup153, and Nup62, but

cleavage of Nup98 appears to occur more rapidly (Park, Katikaneni, Skern, & Gustin, 2008).

NE and NPC-associated Disease States

Cancer

NPCs have a critical function in mitosis, including the assembly and function of kinetochores, mitotic spindles, and centrosomes as well as proper chromosome segregation. This indicates their importance in maintaining genome integrity. Thus, changes that affect the ability of the NPC to function in mitosis could contribute to cancer development (Wong & D'Angelo, 2016). It has been shown that Nup358 (also known as RanBP2), a component of the cytoplasmic filaments of the NPC which functions in multiple cellular processes including mitosis, is implicated in the development of colon cancer (CC), the third most common cancer worldwide. Specifically, Nup358 promotes survival of CC cells by contributing to the prevention of mitotic cell death (Vecchione et al., 2016; Wong & D'Angelo, 2016). A mutation that is observed in about 8-10% of CC patients is the BRAF (V600) mutation, which is typically associated with a less favorable prognosis (Popovici et al., 2012; Vecchione et al., 2016; Wong & D'Angelo, 2016). It has been shown that Nup358 ameliorates the effects of mitotic defects present within BRAF-like CC cell lines. Furthermore, it has been shown that knockdown of the RANBP2 gene leads to mitotic defects in CC cells with this mutation, eventually resulting in cell death specifically due to prolonged mitosis (Hashizume, Kobayashi, & Wong, 2013; Vecchione et al., 2016; Wong & D'Angelo, 2016).

An important feature of nucleocytoplasmic transport through the NPC is the recognition of nuclear localization sequences (NLSs) and nuclear export sequences (NESs) on large proteins by transport receptors. (Mor et al., 2014). Proteins that contain NLSs and NESs include oncogenes and tumor suppressors that have nuclear functions, such as p53 and FoxO. Disruption of nucleocytoplasmic transport involving these proteins is associated with tumor formation (Mor et al., 2014). These proteins bind with Crm1, an exportin, which has been shown to be overexpressed in leukemias, gliomas, and osteosarcomas (Mor et al., 2014). It is believed that this overexpression promotes excessive export of tumor suppressors out of the nucleus, thus decreasing their function (Falini et al., 2005; Mor et al., 2014). Additionally, a mutation in the tumor suppressor gene BRCA2 has been linked to the disruption of nucleocytoplasmic transport. The mutant form of BRCA2 is associated with the development of breast, ovarian, and pancreatic cancers. Interaction of a mutant BRCA2 and the 26S proteasome complex subunit DSS1 has been shown to mask the NES of BRCA2 and allow recognition by Crm1, which mislocalizes it to the cytoplasm (Jeyasekharan et al., 2013; Mor et al., 2014).

One specific Nup, Nup98, regulates transcription of genes that have functions relating to development and the cell cycle (Capelson et al., 2010; Kalverda, Pickersgill, Shloma, & Fornerod, 2010; Mor et al., 2014). Chromosomal translocations involving Nup98 also alter expression of Nup96, as both proteins are encoded by the same mRNA (Fontoura et al., 1999; Mor et al., 2014). Disrupted expression of Nup96 may serve as an additional contributing factor to disease phenotypes that arise from Nup98 translocations with transcription factors, as Nup96 plays a role in the regulation of export of mRNAs that are associated with immunity and cell cycle regulation (Chakraborty et al., 2008; Faria et

al., 2006; Mor et al., 2014). Nup98 translocations are most frequently observed in acute myeloid leukemia (AML), chronic myeloid leukemia in blast crisis (CML-bc), and myelodysplastic syndrome (MDS) (Gough, Slape, & Aplan, 2011). Several mechanisms have been proposed to explain the role of Nup98 fusion proteins in leukemic transformations, including up-regulation of HOXA genes, suppressed differentiation, and increased self-renewal (Gough et al., 2011; Sakuma & D'Angelo, 2017). A study focused on Nup98-HOXA9 revealed a biphasic effect of the fusion protein on the growth of CD34⁺ hematopoietic cells, with growth initially inhibited before continuous, long-term proliferation of primitive cells was observed (Takeda, Goolsby, & Yaseen, 2006). This finding is implicative of the development of AML from MDS, which has been shown in transgenic mouse models containing the fusion protein Nup98-HOXD13. Additionally, Nup98-HOXA9 has been shown to suppress hematopoietic differentiation as well as increase primitive self-renewing cells (Takeda et al., 2006).

Huntington's Disease

Disruption of nucleocytoplasmic transport and the mislocalization and aggregation of several Nups has shown to be involved in Huntington's Disease (HD), the most common heritable neurodegenerative disorder (Grima et al., 2017). HD is a member of a group of neurodegenerative disorders known as polyQ diseases, which are all characterized by repetitive CAG sequences that encode a long polyglutamine (polyQ) tract within corresponding proteins (Finkbeiner, 2011; Grima et al., 2017). There is evidence suggesting that Nup aggregates co-localize with the mutant form of the Huntingtin protein, Htt. Additionally, the number, as well as the size of these aggregates, increase with pathological progression of HD (Grima et al., 2017). Disruption of nucleocytoplasmic

transport as a contributing factor of HD has been demonstrated by disturbance of the Ran gradient. The Ran gradient plays a role in providing power for active transport as well as maintaining proper transport directionality through the interaction of the protein Ran-GTP with the transport receptor during nuclear import. This gradient is maintained by a GTPase-activating protein located on the cytoplasmic filaments of the NPC, RanGAP1 (Floch, Palancade, & Doye, 2014). Interactions between RanGAP1 and RNAs that contain a hexanucleotide repeat expansion (HRE) are linked to disruption of the Ran gradient. These HRE mutations are correlated with some forms of HD and are also commonly seen in amyotrophic lateral sclerosis (ALS) and frontotemporal dementia (FTD) (K. Zhang et al., 2015). Additionally, RanGAP1 and Nup88 have been shown to form aggregates in a mouse model containing HD, and Nup62 has demonstrated severe mislocalization in HD striatum tissue (Grima et al., 2017).

Premature and Accelerated Aging

The NPC is also involved in aging and age-related deterioration. Since aging is a significant risk factor for neurodegeneration, this also demonstrates the role of the NPC in the development of neurodegenerative disorders like HD (Grima et al., 2017). Deterioration occurs by means of molecular damage that builds over time, as Nups have among the greatest longevity of proteins within the mammalian brain (Grima et al., 2017; Savas, Toyama, Xu, Yates, & Hetzer, 2012; Toyama et al., 2013). Nup damage is associated with increased nuclear permeability, which poses the risk of infiltration by toxins and cytoplasmic proteins (D'Angelo, Raices, Panowski, & Hetzer, 2009; Grima et al., 2017). There has been evidence in which leakage of the cytoplasmic protein MAP2 has been observed within *in vitro* models of HD. One study that observed changes in aging

brains of rats revealed that scaffold Nups have very slow turnover rates compared to peripheral Nups, and additionally showed that relative Nup composition of NPCs changed throughout the aging process (Sakuma & D'Angelo, 2017; Toyama et al., 2013). This finding suggests that slow Nup turnover rate may contribute to the accumulation of damaged NPCs over time (Savas et al., 2012).

The nuclear lamina is a supramolecular structure composed of peripheral membrane proteins, which associate with the nucleoplasmic side of the inner nuclear membrane (Gerace & Blobel, 1980). The primary constituents of the lamina are the lamin proteins, which interact with several binding partners through a dense network of filaments (de Leeuw, Gruenbaum, & Medalia, 2018). Lamins are important structural components of the nucleus, as they function in the maintenance of nuclear morphology and stability. It has been shown that lowered lamin expression results in fragile nuclei that are more susceptible to deformation (Broers et al., 2004; Dittmer & Misteli, 2011). Mutations of the lamins are associated with multiple disease states, known collectively as laminopathies, which include muscular dystrophies, lipodystrophies, and peripheral neuropathies (Dittmer & Misteli, 2011). Several of these diseases are caused by mutations in the lamin-encoding gene LMNA, such as Emery-Dreifuss muscular dystrophy, Dunnigan-type familial partial lipodystrophy, and development and accelerated aging disorders including Hutchinson-Gilford Progeria Syndrome (HGPS), a highly rare and fatal premature aging disease (Worman & Bonne, 2007). Additionally, mutations in the genes LMNB1 and LMNB2 are associated with autosomal dominant leukodystrophy and acquired partial lipodystrophy, respectively (Worman & Bonne, 2007). One particular lamin protein, lamin A, is not found in lower organisms like yeast, but its presence is suspected in *C. merolae*.

HGPS is an autosomal dominant disease that results from mutations that arise in the LMNA gene and subsequent malformation of the protein lamin A (Dittmer & Misteli, 2011; Gordon, Rothman, Lopez-Otin, & Misteli, 2014; Gordon et al., 2018). Specifically, single base mutations of the LMNA gene lead to activation of cryptic splice site and subsequent farnesylation of lamin A, producing a variant of the protein known as progerin (Gordon et al., 2018). Continuous farnesylation causes progerin to be incorporated into the inner nuclear membrane, where it amasses and inflicts damage upon aging cells (Gordon et al., 2018). Severe failure to thrive, lipoatrophy, alopecia, skeletal dysplasia, and progressive atherosclerosis are among the symptoms of HGPS. Death typically results from heart attack or stroke at an average age of 14.6 years (Gordon, Cao, & Collins, 2012). Prominent nuclear morphological abnormalities have been observed in HGPS patient cells, including loss of heterochromatin from the nuclear periphery, genomic instability, and premature senescence (Graziano, Kreienkamp, Coll-Bonfill, & Gonzalo, 2018). Furthermore, the normally dynamic lamins are rendered immobilized in the cells of HGPS patients, leading to thickening of the lamina. This triggers changes in the mechanical properties of HGPS nuclei, and these cells thus have greater stiffness as compared to healthy cells. Such modifications in nuclei structure potentially influence the response of cells that are subject to greater mechanical stress including the vasculature, bone, and joints, all of which are affected substantially in the case of HGPS (Gordon et al., 2014).

Research into HGPS may be beneficial in providing insight into the process of generalized aging. The intronic splice site that is activated by the classic HGPS mutation is present in wild-type cells, though infrequently used. Thus, in addition to HGPS, progerin is also generated in the case of normal aging. There has also been evidence to suggest that

the amount of progerin increases correspondingly with age, possibly leading to age-related cellular defects (Gordon et al., 2014; McClintock et al., 2007). Progerin may also have implications on cardiovascular health in relation to normal aging. There have been similarities discovered in atherosclerotic plaques as well as vascular stiffening between the conditions of HGPS and general aging (Gerhard-Herman et al., 2012; Gordon et al., 2014; Olive et al., 2010). However, despite the parallels between HGPS and aging, certain characteristic features of general aging have not been observed in HGPS, including deterioration of the nervous system and deficits of the immune system (Gordon et al., 2014).

Drug treatment with farnesyltransferase inhibitors (FTIs) has shown to be a promising approach to combatting HGPS. FTIs function by reversibly binding to the farnesyltransferase CAAX binding site. Consequently, farnesylation of progerin and following insertion into the nuclear membrane is inhibited (Gordon, Kleinman et al., 2012). A clinical trial conducted by Gordon et al. found that treatment with the FTI lonafarnib correlated with improvements in the rate of weight gain, bone structure, or audiological condition in some patients among a population of 25 children with HGPS (Gordon, Kleinman et al., 2012). Importantly, this study also demonstrated potential benefits of lonafarnib treatment on the cardiovascular system of HGPS patients, including improvement in vascular stiffness (Gordon, Kleinman et al., 2012). Further research has investigated whether lonafarnib treatment has an impact on mortality in children with HGPS (Gordon et al., 2018). Mortality rate of HGPS patients receiving lonafarnib monotherapy was compared with that of patients that received no treatment after 2.2 years

of follow-up. Findings were indicative of an association with a lower mortality rate among patients that received lonafarnib treatment (Gordon et al., 2018).

Changes in lamin expression have demonstrated a link to the development of some cancers, including cancers of the ovary, colon, gut, blood, prostate, lung, and breast (Davidson & Lammerding, 2014). Lamins are involved in multiple pathways with either tumor suppressive or oncogenic roles as well as regulation of apoptosis (Graziano et al., 2018). A-type lamins have been implicated in tumor growth, which is primarily related to their role in the maintenance of nuclear integrity (Graziano et al., 2018). Additionally, both increases and decreases in the expression of lamin A/C have demonstrated an association with aggressiveness of colorectal cancer (Davidson & Lammerding, 2014). A-type lamins also have a function in ensuring the stability of the retinoblastoma tumor suppressor proteins pRb and p107 (Graziano et al., 2018). It has been shown that cancer cell migration through narrow spaces increases with the loss of lamins, which suggests a possible connection between lamins and metastasis (Graziano et al., 2018).

There has been evidence that indicates a possible association between progerin and cancer. For example, a relationship between enhanced tumorigenesis and expression of progerin has been proposed (Graziano et al., 2018; Tang, Chen, Jiang, & Nie, 2010). However, interestingly, while it was initially believed that HGPS patients had a lower cancer risk despite the relationship between aging and cancer due to their shortened lifespan, it has recently been shown that the expression of progerin may potentially protect HGPS cells from malignant transformation. Specifically, BRD4, a bromodomain protein, has been recognized as a mediator of oncogenic resistance within HGPS cells (Fernandez et al., 2014; Graziano et al., 2018).

Objectives

Objective #1 of this study is to isolate and identify protein components of the nuclear pore complex (NPC) from Cyanidioschyzon merolae (C. merolae).

Objective #2 is to visualize and localize individual NPC proteins at the C. merolae NE by immunofluorescence (IF) and confocal microscopy.

Objective #3 is to examine the ultrastructure of C. merolae NPCs by electron microscopy (EM).

Chapter Three

Methods

Objective #1: Isolate and identify protein components of the NPC from C. merolae.

Nuclear Extract Isolation Methods

C. merolae cells were collected for lysis and separation into cytoplasmic and nuclear fractions. Cells were centrifuged and incubated successively in select solutions, with centrifugation between each incubation (See Appendix A for solution preparation).

Following the nuclear extract protocol, the nuclear pellet was resuspended in Solution B and sonicated at 10% amplitude three times at 3-second durations to degrade DNA strands. 1X sample buffer was added to the nuclear pellet and two cytoplasmic fractions. Proteins from whole *C. merolae* cellular extract, nuclear extract, and both cytoplasmic fractions were separated on a 4-20% SDS-PAGE gel and transferred to a nitrocellulose membrane (Bio-Rad Trans-Blot Turbo) for further probing via Western blot analysis.

Western Blotting

Blots were probed with antibodies against several Nups to determine their presence in *C. merolae* and enrichment in the nuclear extract fraction. Blots were blocked overnight in a 5% milk solution in phosphate-buffered saline with Tween (PBS-T) and incubated with primary antibodies in a 2% bovine serum albumin (BSA) for one hour. Blots were then incubated with secondary antibodies in the 5% milk blocking solution for one hour.

5-minute washes with PBS-T were performed between each step. The blots were visualized with electrochemiluminescence (ECL).

Chloroplast Removal and Nuclei Isolation

In order to further isolate the nucleus of *C. merolae*, we employed a chloroplast isolation procedure using a 1X Chloroplast Isolation Buffer (Chloroplast Isolation Kit, ab234623 see Appendix B for preparation). The final Chloroplast Isolation Buffer Solution denoted “Complete Buffer,” was added to 200 mL of *C. merolae* cells, vortexed vigorously in four 30-second increments, and centrifuged at slow speed for 15 minutes. The pellet obtained from this centrifugation contained plant debris, nuclei and whole cells.

After extracting the chloroplasts, we performed an optimized nuclei isolation procedure adapted from a protocol by Sikorskaite et al. (Sikorskaite, Rajamaki, Baniulis, Stanys, & Valkonen, 2013). Samples of 50 μ L were collected following each fractionation step in order to track the location of the nuclei. We obtained 200 mL of *C. merolae* cells, collected a 50 μ L sample of untreated cells which was stored on ice, and performed a chloroplast removal procedure as described previously. A 50 μ L sample was collected from the supernatant and stored on ice. The pellet was resuspended in 1 mL of Storage Buffer (see Appendix C), and a 50 μ L sample was collected and stored on ice. 10% Triton X-100 was added to the solution to reach a concentration of 0.5%. The solution was lightly agitated for 20 minutes at 4°C, followed by centrifugation at slow speed for 10 minutes. A 50 μ L sample was collected from the supernatant and stored on ice. The pellet was resuspended in 10 mL of Storage Buffer. The solution was dispensed over a density gradient that was comprised of 5 mL of 60% Percoll (GE Healthcare, 45001747) solution

on top of 5 mL of a 2.5 M sucrose bed. The gradient was centrifuged at slow speed for 30 minutes at 4°C. A 50 µL sample was collected from each layer and stored on ice. The Percoll layer, which contained nuclei, was diluted with 5 volumes of storage buffer and 0.5% Triton-X 100. This solution was lightly agitated for 20 minutes at 4°C, followed by centrifugation at slow speed for 10 minutes. A 50 µL sample was collected from the supernatant and stored on ice. The pellet was diluted with 5 volumes of storage buffer and 0.5% Triton-X 100, and lightly agitated followed by centrifugation as previously described. A 50 µL sample was collected from the supernatant and stored on ice. The pellet was resuspended in 5 mL of Storage Buffer and dispensed over 5 mL of 35% Percoll solution, followed by centrifugation at slow speed for 10 minutes at 4°C. A 50 µL sample was collected from the supernatant and stored on ice. The pellet was resuspended in 200 µL of Storage Buffer, a 50 µL sample was collected and stored on ice. 20 µL of each sample was loaded onto 4-well microchamber slides sequentially in the order that they were obtained. The samples were mixed with 1000X DAPI (diluted to 1X) and allowed to dry, then mounted with cover slips. These slides were used for analysis by immunofluorescence.

Proteomics

C. merolae samples were sent to NYU Langone's Proteomics Laboratory. Proteomic screening for Nups was carried out using gel digestion and peptide extraction approach. Peptides were separated by liquid chromatography (LC) and gradient eluted from the column directly to an Orbitrap Elite mass spectrometer using a 1-hour gradient (Thermo Scientific). High-resolution full MS spectra were acquired and searched against a *C. merolae* database (UniProtKB Proteome ID UP000007014).

Objective #2 : Visualize and localize individual NPC proteins by immunofluorescence (IF) and confocal microscopy.

Immunofluorescence, Confocal Microscopy, and Live Cell Imaging

IF was performed using an Echo Revolve Fluorescent Microscope to visualize the nuclear localization of Nups identified as positive in *C. merolae*. *C. merolae* cells were placed in a 4-well microchamber slide and suspended and fixed in 3% formaldehyde. Cells were then incubated in 0.05% Triton X-100 (MP, 194854) for 15 minutes, which was followed by blocking with 5% BSA for 30 minutes. Brief washes with PBS were performed between each step. Cells were incubated with primary antibodies in 2% BSA for 2 hours followed by incubation with a fluorescein-conjugated secondary IgG antibody for 2 hours. Washes with 2% BSA were formed between incubation steps. The cells were then mounted onto the slides with DAPI.

C. merolae cells were imaged by confocal microscopy using the Zeiss LSM 880 Confocal Laser Scanning Microscope with Airyscan. Live cell imaging of unsynchronized cells was performed using parameters of 42°C and 5% CO₂. Cells were grown in a glass bottom dish with a #1.5 glass cover slip (Cellvis, #D35-20-1.5-N). Directly before imaging, cells were incubated with Hoechst 33258 (Invitrogen, #H3569), which was diluted to a concentration of 0.1 µg/mL, for 1 hour and 30 minutes at 42°C. 2 µL of Hoechst dye was added to 2 mL of cells to reach a final concentration of 0.1 µg/mL. Chloroplast and DNA signals were visualized using excitation wavelengths of 561 nm and 405 nm, respectively. Cells were imaged at a rate of 1 scan per minute over the course of 1 hour to obtain a total of 60 frames.

ER/Mitochondria Labeling

In order to further characterize the internal structures of *C. merolae* to better understand the structure of the NPC, the ER and mitochondria of *C. merolae* were visualized by employing dye labeling techniques. *C. merolae* cells were isolated by centrifugation and incubated in a 1 μ M solution of ER-Tracker Green (Thermo Fisher Scientific ER-Tracker™ Green E34251) in PBS at 42°C. ER-Tracker Green is highly selective for the ER (Hogg & Adams, 2001). To determine an incubation time for optimal uptake of labeling dye, cells were incubated over the following time periods 0 minutes, 30 minutes, 60 minutes, and 90 minutes. After each time point, cells were centrifuged and washed with PBS. Cells were resuspended in PBS and mounted onto slides with DAPI. This procedure was repeated using MitoTracker Green FM (Thermo Fisher Scientific MitoTracker™ Green FM, M7514), a green-fluorescent dye that has been shown to localize to mitochondria (Samudio et al., 2005).

Images of *C. merolae* stained with DAPI and ER Green or MitoTracker Green FM were acquired via IF (EchoRevolve) according to the following protocol. 5 randomly positioned images were taken per time point of the stained cells (30, 60, 90 min.) using the 20x objective lens under the FITC setting (96% brightness, HI gain, 2695 ms exposure). Pixels were counted using Adobe Photoshop CC 2017. Pixel counts were taken for all 5 images per time point for both ER Green and MitoTracker Green FM stained *C. merolae* cells. Descriptive statistics were calculated, and comparisons between stains at different time points were analyzed for statistical differences via independent Student's t-tests ($\alpha = 0.1$). F-tests were used to determine whether the t-tests should be computed assuming equal or unequal variances. MitoTracker Green FM-stained cells showed the greatest staining

capacity at 90 minutes with significant differences from 30 and 60 minutes, respectively, at a 95% confidence level (1-tailed test). ER Green-stained cells also exhibited the greatest staining capacity at 90 minutes and showed a significant difference between 90 and 30 minutes (1-tailed test) but not between 90 and 60 minutes. However, to maintain consistency between the two stains, it was determined that 90 minutes should be used as the incubation time for both stains. We confirmed our IF data by conducting additional analyses using confocal microscopy.

Objective #3: Examine the ultrastructure of *C. merolae* NPCs by electron microscopy (EM).

Electron Microscopy

High-resolution imaging was carried out to determine the feasibility of analyzing the ultrastructure of NPCs within *C. merolae* via EM. This work was done through collaboration with the Beck Lab at the European Molecular Biology Laboratory in Heidelberg, Germany. EM samples at a concentration of $1-4 \times 10^6$ cells per ml were prepared (Schaffer et al., 2015). Cell concentration was determined by counting using a hemocytometer. Carbon-coated 200-mesh copper transmission electron microscopy (TEM) grids were placed on a glass slide with the carbon side facing up, and glow discharged by 30-second plasma cleaning (Schaffer et al., 2015). The cells were plunge-frozen using the Vitrobot biochamber, which was set to 90% humidity, blot force 10, 7, to 10 second blot time. Inside the Vitrobot, 3.5 μL of the diluted cell culture was pipetted onto TEM grids. The grids were blotted from with Teflon sheets on both sides, and filter

paper on the backside. They were immediately plunged into the liquid ethane/propane mixture at liquid nitrogen temperature (Schaffer et al., 2015).

Focused ion beam (FIB) milling was used to produce thin, distortion-free lamellae material for high-resolution cryo-ET. Focused ion beam/scanning electron microscope system initially visualize algae in clumps by scanning electron microscopy (SEM). Further, electron microscopic data were acquired using a Titan Krios TEM (FEI), equipped with Gatan Camera and GIF 2002 energy filter (Gatan) (Beck & Hurt, 2017; Knockenhauer & Schwartz, 2016; Mosalaganti et al., 2018; Schaffer et al., 2015).

Chapter Four

Results

Nuclear Isolation

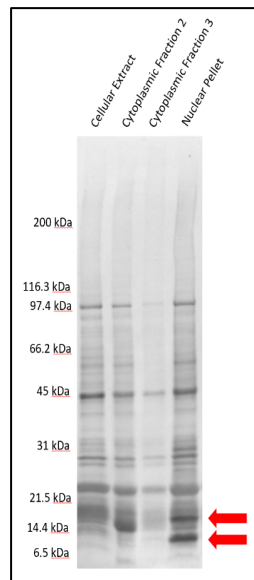


Figure 3

C. merolae nuclear extract gel transfer. Lane 1. *C. merolae* cellular extract, Lane 2. cytoplasmic fraction 2, Lane 3. cytoplasmic fraction 3 and Lane 4. nuclear extract pellet were separated on 4–20 % SDS-PAGE and stained with Amido Black.

The gel transfer, which was stained non-specifically for proteins with Amido Black (AlfaAesar, 1064-48-8), from *C. merolae* cellular extract, nuclear extract, and cytoplasmic fractions is shown in Figure 3. We expect that the intense bands indicated by red arrows are showing enrichment of histones, which are associated with the NE (Cronshaw et al., 2002).

The results from probing with all of the antibodies tested by Western blotting are summarized in Table 1. Our data indicate reactivity to antibodies against Nups including

Sec13, Nup43, and Nup96, symmetric nucleoporins that form the core region of the NPC, as well as ELYS (Figure 4). (Hoelz, Debler, & Blobel, 2011). This demonstrates their presence in *C. merolae*.

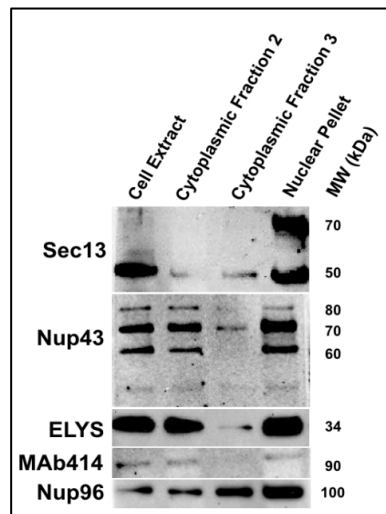


Figure 4

Western blotting of antibodies against several Nups and MAb414 in *C. merolae* whole cell extract, cytoplasmic fractions 2 and 3, and nuclear extract.

Positive Reaction	Negative Reaction
Anti-Lamin A/C	Anti-Nup54
Anti-Lamin B1	Anti-Nup62
Anti-Calnexin	Anti-Actin
Anti-Nup50	Anti-alpha Tubulin
Anti-Nup88	Anti-RAN
Anti-NDC1	Anti-Nup155
Anti-Nup107	Anti-Synuclein
Anti-ELYS	Anti-Mab414
Anti-Nup96	Anti-NupL2
Anti-TPRN	Anti-Nup93 N-terminus
Anti-Sec13	Anti-Nup93 C-terminus
Anti-Nup160	Anti-Nup214
Anti-Nup43	Anti-gp210
Anti-Nup153	Anti-LAP2
Anti-Wheat Germ Agglutinin	Anti-POM33
Anti-O-linked <i>N</i> -acetylglucosamine	

Table 1

Antibodies tested by Western blotting that generated positive or negative reactions.

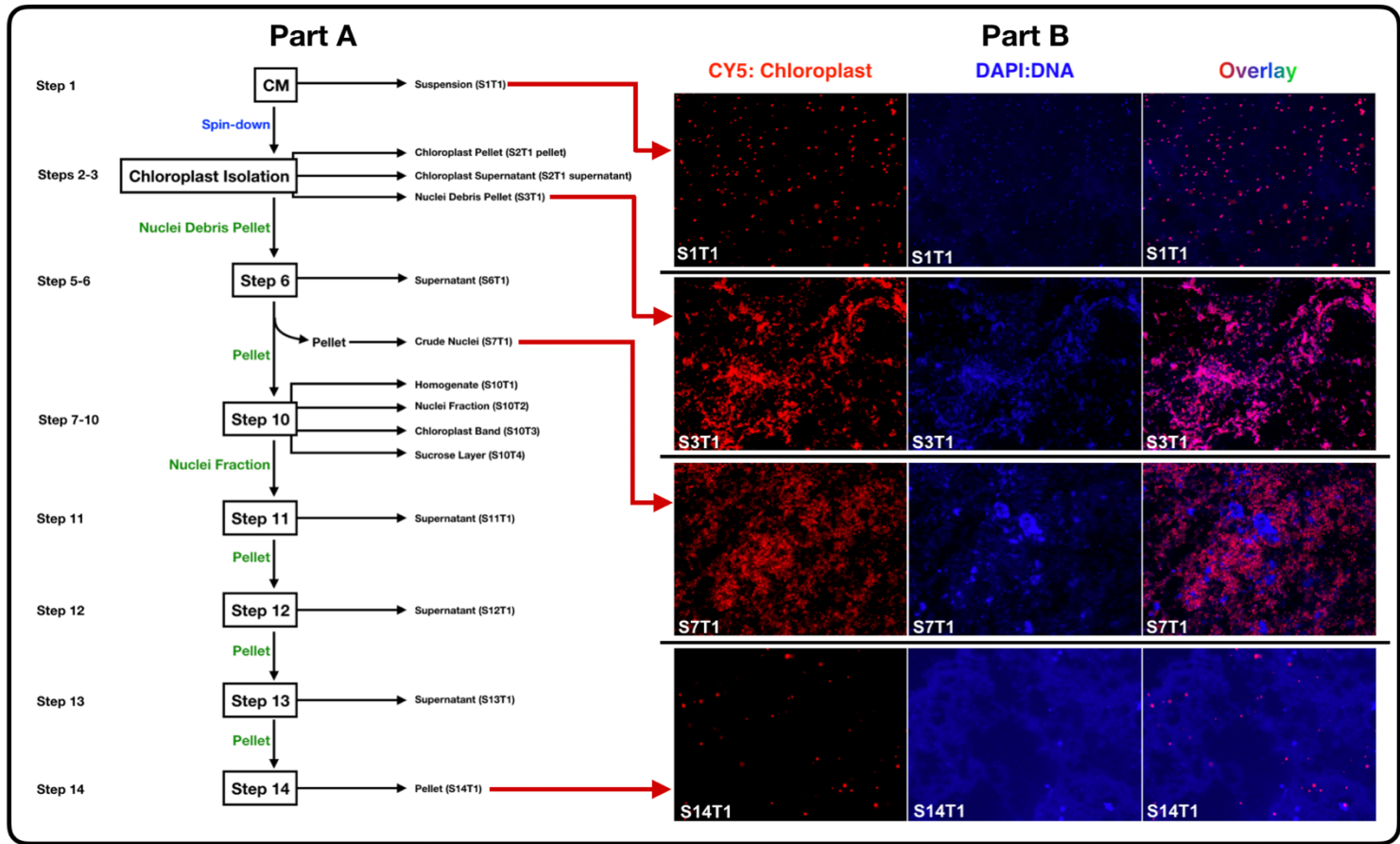


Figure 5

Flow chart illustrating each step of the fractionation process by which nuclei was isolated and samples collected at each step (A). Immunofluorescent microscopy analysis of samples S1T1, S3T1, S7T1, and S14T1 following the optimized nuclei isolation (B).

The steps at which samples were collected through the optimized nuclei isolation procedure are shown in Figure 5A. We analyzed each sample by immunofluorescent microscopy to track the nuclei throughout fractionation as well as determine the extent to which the chloroplasts were being separated out. Chloroplasts were visualized by their auto-fluorescent properties. DAPI (Thermo Fisher ProLong™ Gold Antifade Mountant with DAPI, P36935) was used to stain DNA, which allowed for tracking of the nuclei.

Figure 5B shows IF images of S1T1, which contained untreated *C. merolae* cells; S3T1, which contained debris, nuclei and whole cells following the chloroplast removal procedure; S7T1, which contained crude nuclei prior to extraction through the density gradient; and S14T1, which contained the final nuclear product. There is a clear reduction in chloroplasts in S14T1 compared to S1T1.

Proteomics

The gel digestion and peptide extraction methods used for proteomic screening for Nups within *C. merolae* nuclear extract are summarized in Figures 6 and 7.

We successfully identified 13 Nups within a sample of *C. merolae* nuclear extract by proteomic analysis. The main criterion for Nup identification was that at least 5 peptides had to be detected. The only exception was POM33, for which 2 peptides were detected. However, it was expected that there would be fewer peptides detected for this particular protein, as it is a transmembrane Nup. Since Nups of this group are actually embedded within the nuclear membrane, they are traditionally more difficult to digest.

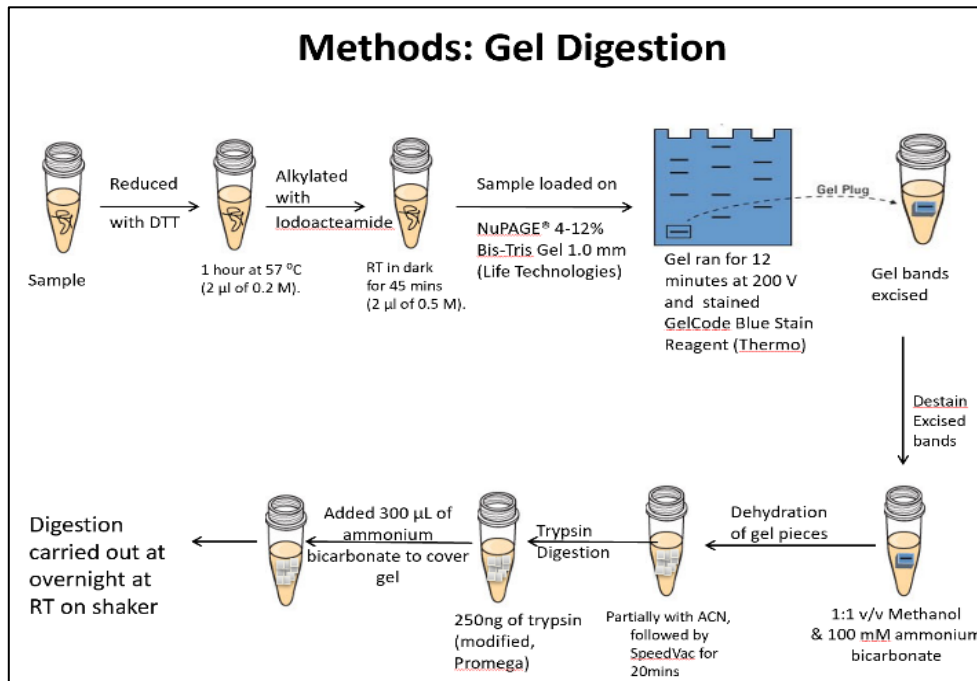


Figure 6
Summary of gel digestion methods used for proteomic analysis of *C. merolae*.

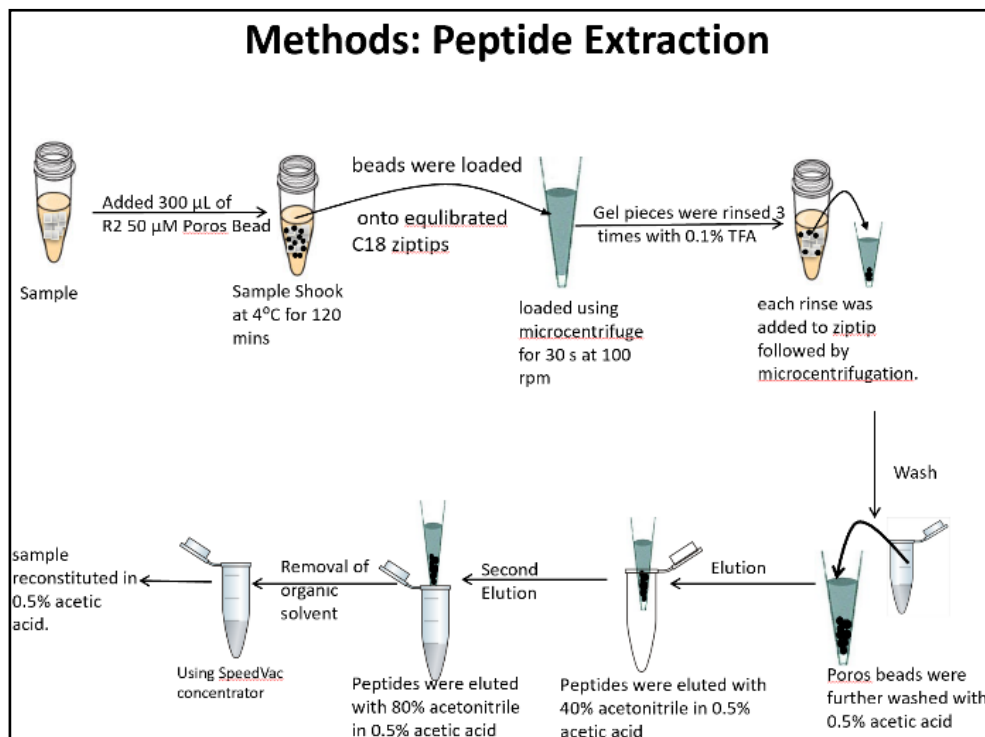


Figure 7
Summary of peptide extraction methods used for proteomic analysis of *C. merolae*.

Nup	UniProt ID	<i>C. merolae</i> Reference Genome
Nup107	M1V6L8	CYME_CMC129C
Nup93	M1V6Q4	CYME_CMR125C
Nup98	M1VEJ0	CYME_CMB112C
Nup133	M1VAI5	CYME_CMQ238C
Nup155	M1VBS8	CYME_CMH179C
Rae1	M1UQZ1	CYME_CMI077C
Sec13	M1VCG0	CYME_CMJ112C
Nup50	M1UQP9	CYME_CMH178C
Nup58/45	M1UWR3	CYME_CMS092C
Pom33	M1V6S5	CYME_CMR216C
Nup2	M1VEJ0	CYME_CMB112C
Nup62	M1UVA1	CYME_CMP228C
Nup96	M1V6H0	CYME_CMB113C

Table 2

Nups identified by proteomics in *C. merolae* nuclear extract.

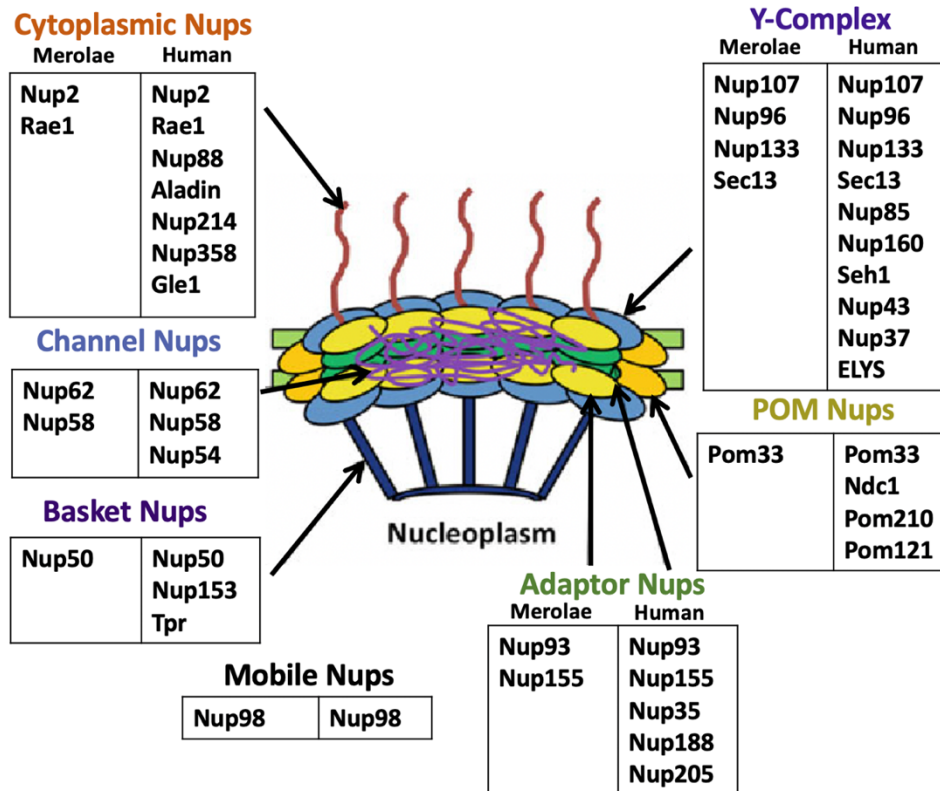


Figure 8

Nups identified by proteomics in *C. merolae* nuclear extract, categorized by major group and compared to known Nups in humans within each respective group. The location of each Nup type within the NPC is also indicated.

Immunofluorescence and Confocal Microscopy

By IF, we have observed reactivity to the NPC-associated proteins Nup107 and NDC1 in *C. merolae*. We also probed for KDEL, an ER-associated protein, in order to compare localization. These findings (summarized in Figure 9) were confirmed by super-resolution confocal microscopy.

Additionally, we have visualized the ER and mitochondria in *C. merolae*. Confocal analysis of these structures is summarized in Figure 10. We observed a distinction between the ER and nuclear membranes, as demonstrated by the physical separation between the green- and blue-stained regions of the cell.

We were able to observe the movement of *C. merolae* cells through the visualization of their auto-fluorescent chloroplasts and Hoechst-stained DNA. We generated images taken at a total of 60 time points over the course of 1 hour. A sample of 3 consecutive time points is shown in Figure 11.

Electron Microscopy

Initial experiments conducted using SEM revealed aggregations of *C. merolae* cells, and mitotic cells could be distinguished by their larger size (Figure 12). We observed the lamellar surfaces of the chloroplast as well as the nucleus and double membrane. The chloroplast was the most prominent structure that was visible, and it appeared to hug the nucleus (Figure 13).

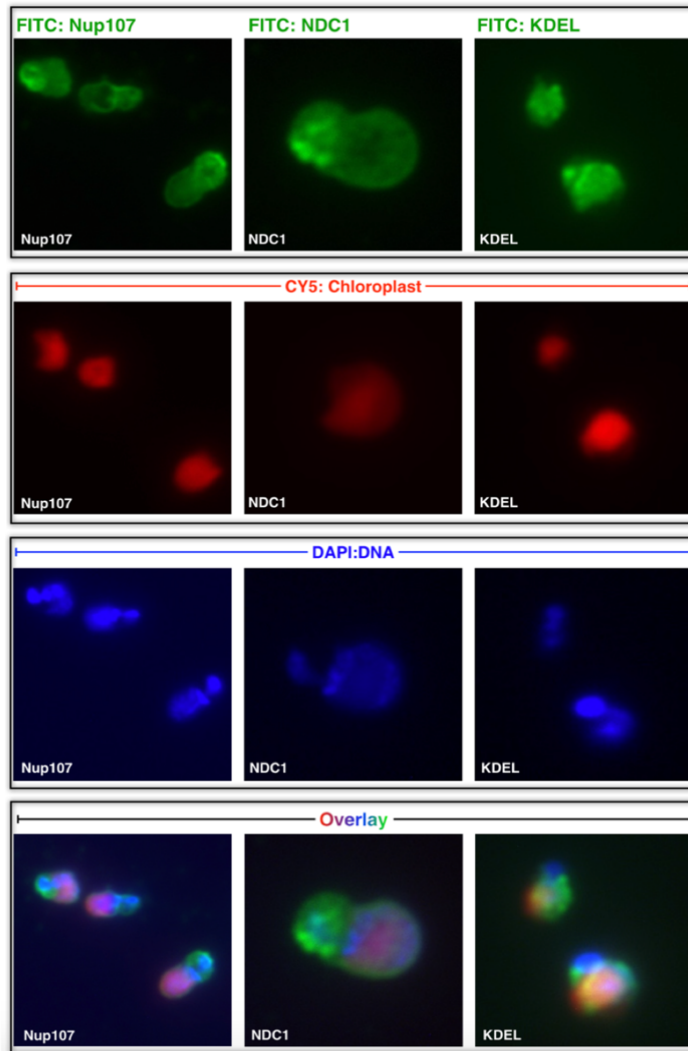


Figure 9

Immunofluorescent microscopy analyses of NE-associated proteins including Nup107 and NDC1 as well as the ER-associated protein KDEL in *C. merolae*.

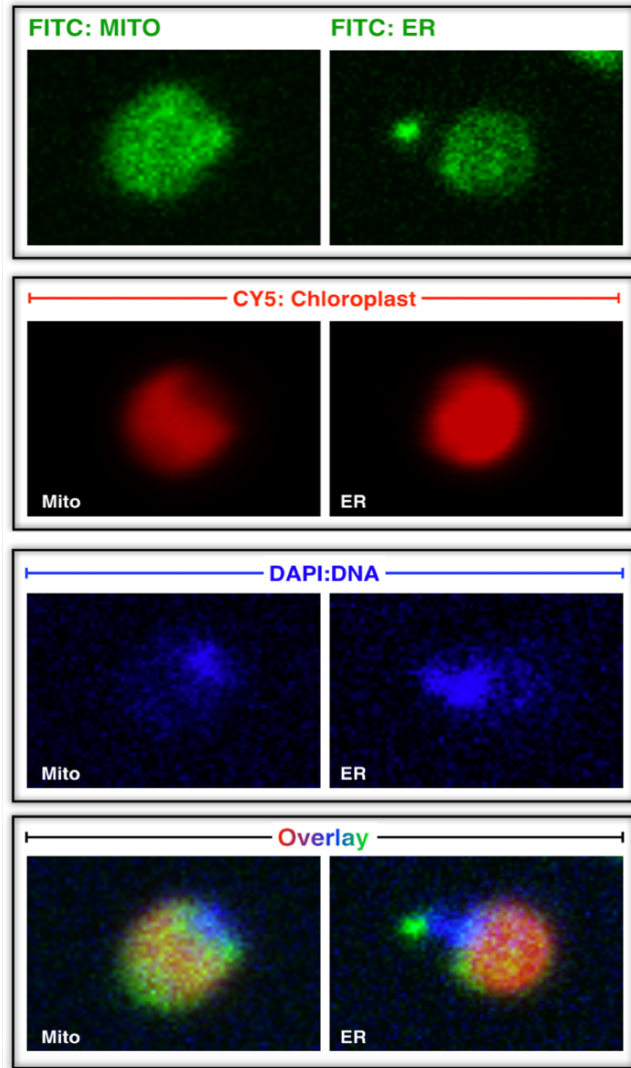


Figure 10

Confocal microscopy analyses *C. merolae* cells labeled with ER and mitochondria dyes.

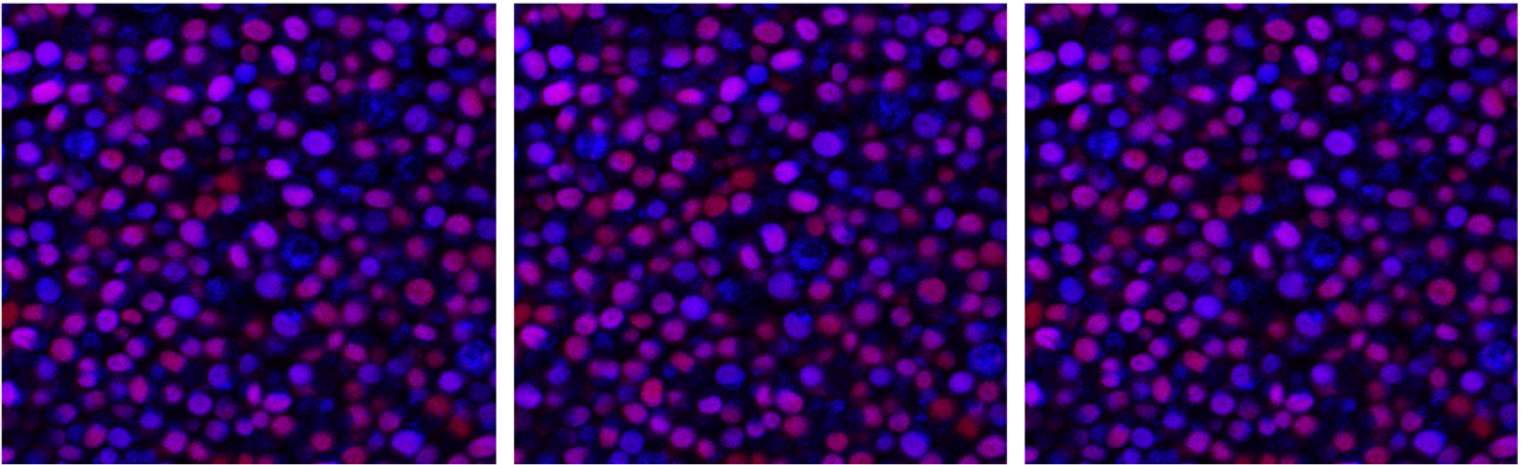


Figure 11

Live cell images of *C. merolae* at time points 26-28, each taken 1 minute apart. Chloroplasts were visualized by their auto-fluorescence (red), and DNA was visualized by Hoechst-staining (blue).

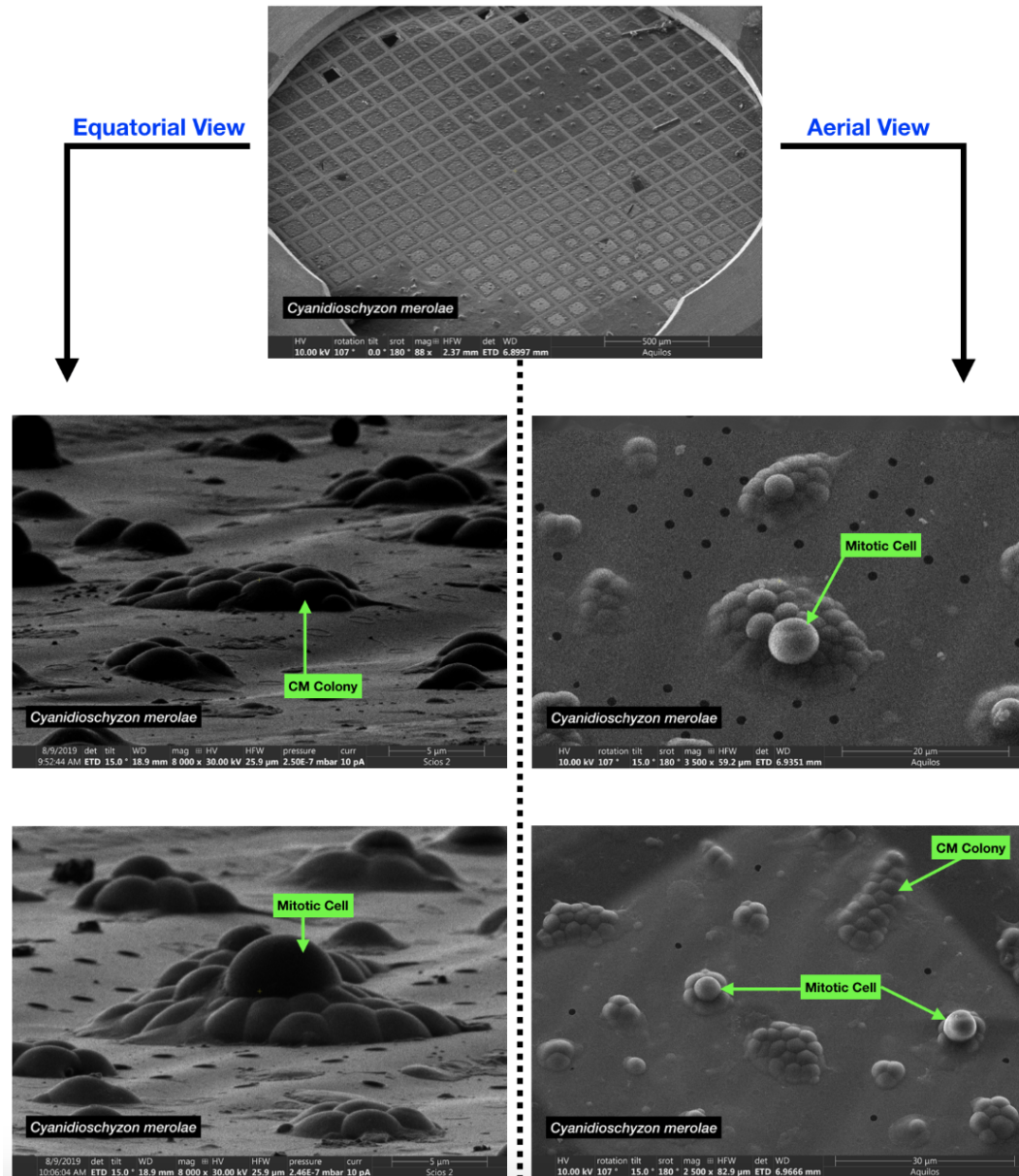


Figure 12

Scanning electron microscopy analyses of the external surface of *C. merolae* cells. Overview of the TEM grids (top center), equatorial views (left), and aerial views (right). Mitotic cells are also indicated.

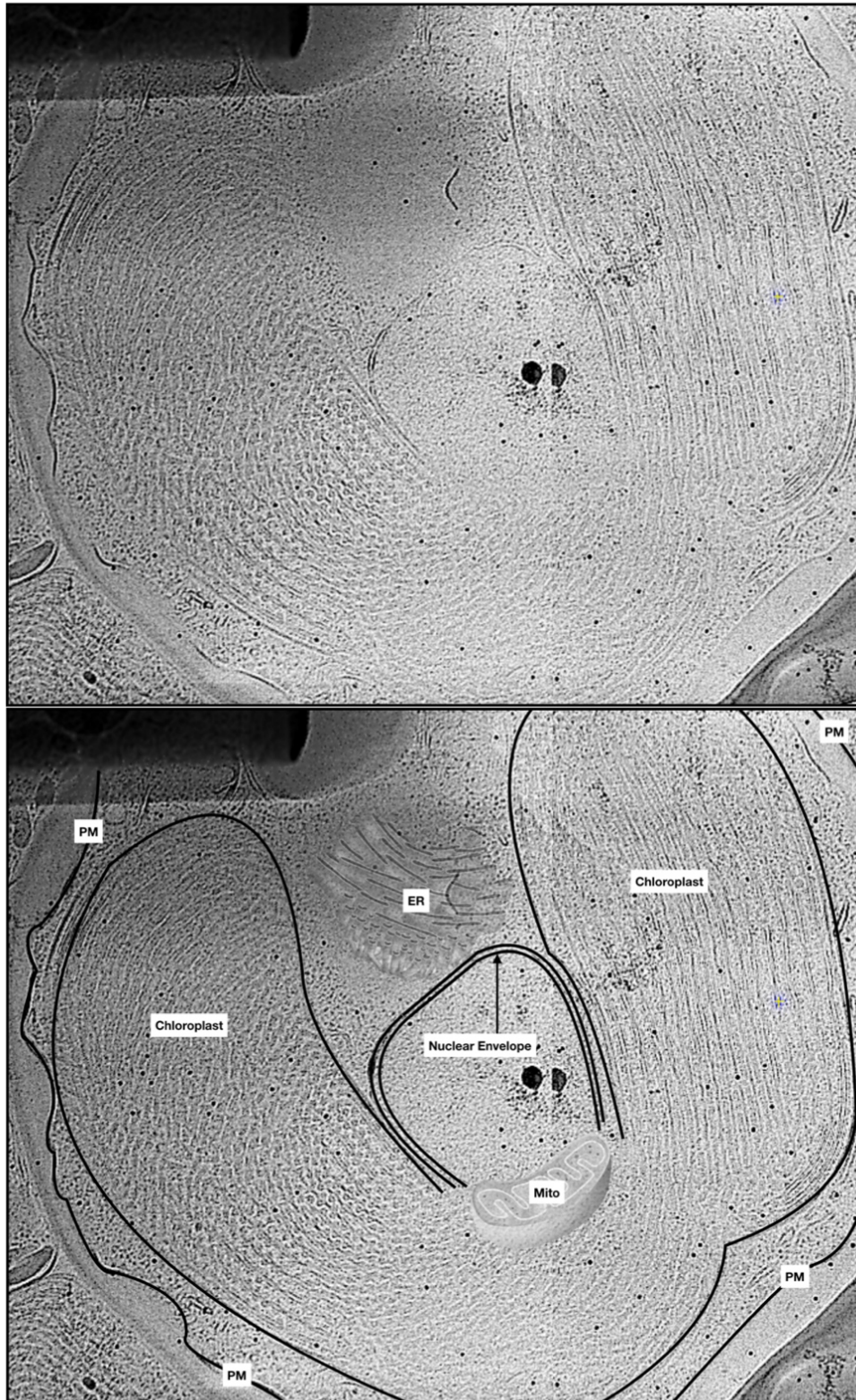


Figure 13

Transmission electron microscopy analysis of *C. merolae*. Visible structures are indicated in bottom panel, including the plasma membrane (PM), the chloroplast, the nuclear envelope, and the ER. Probable location of the mitochondria is also shown.

Chapter Five

Discussion

The proteomic composition of the NPC in *C. merolae* has not previously been well characterized. Initial nuclear isolation techniques performed with *C. merolae* resulted in the enrichment of DNA with histones, which confirmed that we had obtained a mostly nuclear pellet. While treatment by DNase and RNase was applied to reduce the presence of nucleic acids, they were not entirely eliminated from the final product. Additional methods to lessen histone content should be incorporated into this procedure, such as heparin treatment. Our further optimized nuclei isolation procedure demonstrated a reduction in chloroplast content within *C. merolae*, while the nuclei were still maintained (Figure 5). While the final product did appear to contain an overall lower nuclei content, this limitation could be addressed by upscaling the starting material. In addition, the fractionated nuclear product should be treated with DNase and RNase in future experiments to reduce the nucleic acid content.

When probing by Western blot analysis, we used antibodies against human Nups to determine what cross-reactivity would occur. We visualized Nups that had previously been predicted in *C. merolae*, which included Sec13, Nup50, Nup88, Nup107, and Nup96 (Table 1). Additionally, we observed cross-reactivity with Nups that had not been predicted in *C. merolae*, which included Lamin A/C, Lamin B1, NDC1, TPRN, Nup160, Nup43, Nup153, and ELYS (Table 1). We also visualized Wheat Germ Agglutinin and *O*-linked *N*-acetylglucosamine, a lectin and intracellular carbohydrate, respectively, that are added to human Nups, indicating that this modification also occurs in *C. merolae* (Table 1). Proteomic analysis identified a total of 13 Nups out of 20 that are predicted within the

nuclear extract of *C. merolae*, with at least 1 identified from each major group (Figure 8). There may still be more Nup members yet to discover that could potentially be specific to *C. merolae*. This could explain why some Nups, such as NDC1, demonstrated cross-reactivity by Western blotting but were not identified by proteomics. Nups for which cross-reactivity was observed that were not predicted can be isolated by immunoisolation followed by proteomics. This would allow these proteins/peptides to be identified through sequencing and more complex bioinformatics analysis in order to build an inventory of the NPC in *C. merolae*.

Imaging by fluorescent and confocal microscopy allowed for visualization of nuclear rim staining of Nups from two different groups: Nup107, a member of the Y-complex group; and NDC1, a member of the POM group, which exhibited round rim staining. Additionally, DAPI staining allowed for visualization of three different groups of DNA within *C. merolae*: nuclear DNA, mitochondrial DNA, and chloroplast DNA (Figure 9). Most of the DNA observed originated from the nucleus. We also probed for the presence of KDEL, a sequence known to be found exclusively in the ER (Figure 10). Localization of KDEL as well as ER and mitochondria staining demonstrated a distinction between nuclear DNA from the other cellular components. Using confocal techniques, we successfully performed live cell imaging with *C. merolae* cells, which demonstrates the potential for using this type of analysis on this species. This method could have incredible utility for future research goals, such as the analysis of *C. merolae*'s cell cycle.

EM findings established the feasibility of visualizing the ultrastructure of the NPC within *C. merolae*. Initial experiments conducted using SEM revealed the presence of *C. merolae* cells in clumps. This behavior is an advantageous characteristic, as this simplifies

further analysis by TEM. TEM analysis revealed that the NPCs were not visible within the images we captured, which was likely due to their small size and a possibility of low abundance. However, we still observed a relatively full spectrum of morphology in *C. merolae*, including the lamellar surfaces of the chloroplast as well as the nucleus and double membrane. Notably, the chloroplast was shown to hug the nucleus, which may have functional implications such as communication and protection. In addition, these findings demonstrated the ability to designate mitotic cells, which has important implications on potential cell cycle studies. More EM data on *C. merolae* is needed to definitively determine its structural constitution.

The time points at which we expected to complete our three specific aims over the course of a two-year project are outlined in Figure 14. We have completed Specific Aim #1 through successful nuclear isolation of *C. merolae*, which allowed for proteomic identification of Nups from every major group. This elucidated the protein composition of the NPC in *C. merolae*. We also demonstrated the ability to reduce the chloroplast content within *C. merolae*, an important method by which the process of nuclear isolation may be augmented. Furthermore, we have observed the presence of several NPC proteins in *C. merolae* by Western blotting. As part of Specific Aim #2, we have visualized the localization of NPC proteins in *C. merolae* via IF. We have also characterized structural features of *C. merolae* including the ER and mitochondria by IF as well as confocal microscopy and additionally demonstrated the ability to perform live cell imaging. This data showed that there is a clear separation of the NE from the ER, which is significant since previous work has described more of an association between these membranes. This finding will facilitate a more comprehensive understanding of *C. merolae*'s NE and NPC.

We have made considerable progress towards visualization of the ultrastructure of the NPC in *C. merolae* by EM (Specific Aim #3), as we have successfully employed both SEM and TEM techniques.

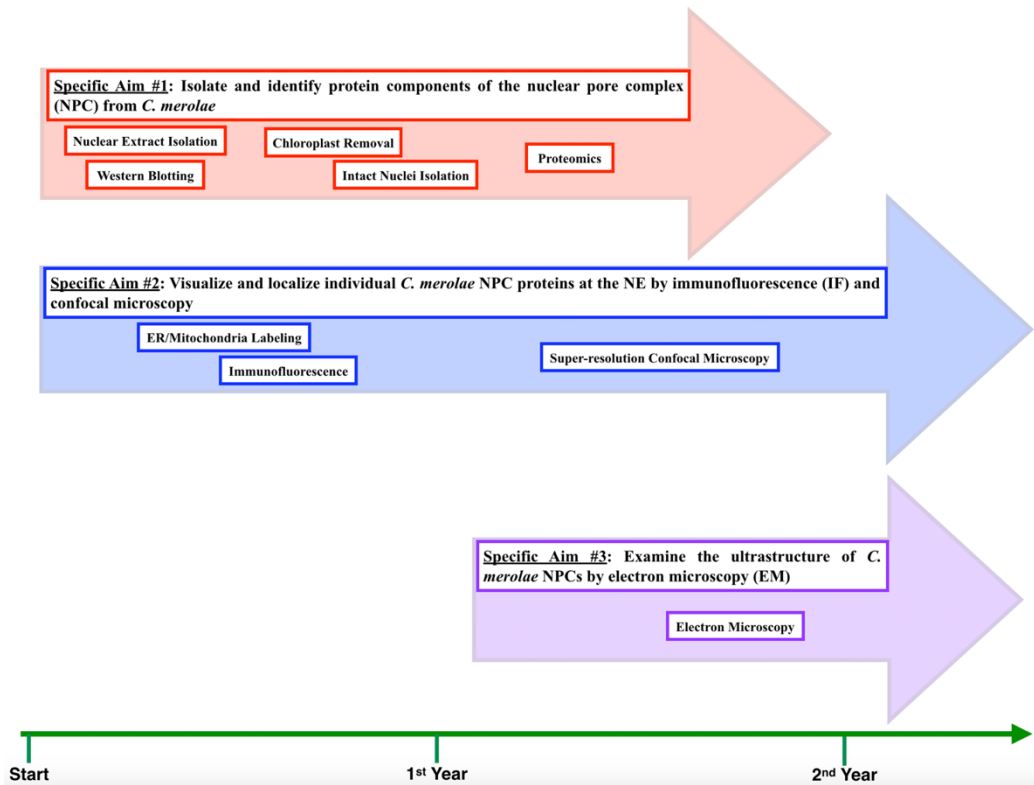


Figure 14
Expected timeline to complete specific aims of project.

Characterization of *C. merolae*'s NPC could implicate *C. merolae* as an unexploited resource for determining new answers about a variety of disease states, potentially providing a more accurate representation of pathological processes. Nups are associated

with several different forms of cancer, neurodegenerative diseases such as Huntington's Disease, and premature aging diseases such as Hutchinson-Gilford Progeria Syndrome. Additionally, disruption of transport through the NPC has been linked to conditions such as breast cancer. Thus, *C. merolae* could be utilized as an ideal model system to study a number of disease types as well as multiple mechanisms of progression.

References

- Aaronson, R. P., & Blobel, G. (1974). On the attachment of the nuclear pore complex. *J Cell Biol*, 62(3), 746-754. Retrieved from <https://www.ncbi.nlm.nih.gov/pubmed/4853439>.
- Alber, F., Dokudovskaya, S., Veenhoff, L. M., Zhang, W., Kipper, J., Devos, D., . . . Sali, A. (2007). Determining the architectures of macromolecular assemblies. *Nature*, 450(7170), 683-694. Retrieved from http://www.ncbi.nlm.nih.gov/entrez/query.fcgi?cmd=Retrieve&db=PubMed&dopt=Citation&list_uids=18046405. doi:nature06404 [pii] 10.1038/nature06404
- Antonin, W., Ellenberg, J., & Dultz, E. (2008). Nuclear pore complex assembly through the cell cycle: regulation and membrane organization. *FEBS Lett*, 582(14), 2004-2016. Retrieved from http://www.ncbi.nlm.nih.gov/entrez/query.fcgi?cmd=Retrieve&db=PubMed&dopt=Citation&list_uids=18328825. doi:S0014-5793(08)00190-7 [pii] 10.1016/j.febslet.2008.02.067
- Antonin, W., & Mattaj, I. W. (2005). Nuclear pore complexes: round the bend? *Nat Cell Biol*, 7(1), 10-12. Retrieved from <http://www.nature.com/ncb/journal/v7/n1/abs/ncb0105-10.html>
- Beck, M., Forster, F., Ecke, M., Plitzko, J. M., Melchior, F., Gerisch, G., . . . Medalia, O. (2004). Nuclear pore complex structure and dynamics revealed by cryoelectron tomography. *Science*, 306(5700), 1387-1390. Retrieved from http://www.ncbi.nlm.nih.gov/entrez/query.fcgi?cmd=Retrieve&db=PubMed&dopt=Citation&list_uids=15514115. doi:1104808 [pii] 10.1126/science.1104808
- Beck, M., & Hurt, E. (2017). The nuclear pore complex: understanding its function through structural insight. *Nat Rev Mol Cell Biol*, 18(2), 73-89. Retrieved from <https://www.ncbi.nlm.nih.gov/pubmed/27999437>. doi:10.1038/nrm.2016.147
- Beck, M., Lucic, V., Forster, F., Baumeister, W., & Medalia, O. (2007). Snapshots of nuclear pore complexes in action captured by cryo-electron tomography. *Nature*, 449(7162), 611-615. Retrieved from http://www.ncbi.nlm.nih.gov/entrez/query.fcgi?cmd=Retrieve&db=PubMed&dopt=Citation&list_uids=17851530. doi:nature06170 [pii] 10.1038/nature06170
- Belgareh, N., Rabut, G., Bai, S. W., van Overbeek, M., Beaudouin, J., Daigle, N., . . . Doye, V. (2001). An evolutionarily conserved NPC subcomplex, which redistributes in part to kinetochores in mammalian cells. *J Cell Biol*, 154(6), 1147-1160. Retrieved from http://www.ncbi.nlm.nih.gov/entrez/query.fcgi?cmd=Retrieve&db=PubMed&dopt=Citation&list_uids=11564755.
- Boehmer, T., Enninga, J., Dales, S., Blobel, G., & Zhong, H. (2003). Depletion of a single nucleoporin, Nup107, prevents the assembly of a subset of nucleoporins into the nuclear pore complex. *Proc Natl Acad Sci U S A*, 100(3), 981-985. Retrieved from

http://www.ncbi.nlm.nih.gov/entrez/query.fcgi?cmd=Retrieve&db=PubMed&dopt=Citation&list_uids=12552102. doi:10.1073/pnas.252749899252749899 [pii]

- Boehmer, T., Jeudy, S., Berke, I. C., & Schwartz, T. U. (2008). Structural and functional studies of Nup107/Nup133 interaction and its implications for the architecture of the nuclear pore complex. *Mol Cell*, *30*(6), 721-731. Retrieved from http://www.ncbi.nlm.nih.gov/entrez/query.fcgi?cmd=Retrieve&db=PubMed&dopt=Citation&list_uids=18570875. doi:S1097-2765(08)00325-0 [pii] 10.1016/j.molcel.2008.04.022
- Boettcher, B., & Barral, Y. (2013). The cell biology of open and closed mitosis. *Nucleus*, *4*(3), 160-165. Retrieved from <http://www.ncbi.nlm.nih.gov/pubmed/23644379>. doi:10.4161/nucl.24676
- Bonny, D. P., Hull, M. L., & Howell, S. M. (2014). Design, calibration and validation of a novel 3D printed instrumented spatial linkage that measures changes in the rotational axes of the tibiofemoral joint. *J Biomech Eng*, *136*(1), 011003. Retrieved from <http://www.ncbi.nlm.nih.gov/pubmed/24064860>. doi:10.1115/1.4025528
- Broers, J. L., Peeters, E. A., Kuijpers, H. J., Endert, J., Bouten, C. V., Oomens, C. W., . . . Ramaekers, F. C. (2004). Decreased mechanical stiffness in LMNA-/- cells is caused by defective nucleo-cytoskeletal integrity: implications for the development of laminopathies. *Hum Mol Genet*, *13*(21), 2567-2580. Retrieved from <https://www.ncbi.nlm.nih.gov/pubmed/15367494>. doi:10.1093/hmg/ddh295
- Bui, K. H., von Appen, A., DiGuilio, A. L., Ori, A., Sparks, L., Mackmull, M. T., . . . Beck, M. (2013). Integrated structural analysis of the human nuclear pore complex scaffold. *Cell*, *155*(6), 1233-1243. Retrieved from <https://www.ncbi.nlm.nih.gov/pubmed/24315095>. doi:10.1016/j.cell.2013.10.055
- Capelson, M., Liang, Y., Schulte, R., Mair, W., Wagner, U., & Hetzer, M. W. (2010). Chromatin-bound nuclear pore components regulate gene expression in higher eukaryotes. *Cell*, *140*(3), 372-383. Retrieved from <https://www.ncbi.nlm.nih.gov/pubmed/20144761>. doi:10.1016/j.cell.2009.12.054
- Chadrin, A., Hess, B., San Roman, M., Gatti, X., Lombard, B., Loew, D., . . . Doye, V. (2010). Pom33, a novel transmembrane nucleoporin required for proper nuclear pore complex distribution. *J Cell Biol*, *189*(5), 795-811. Retrieved from http://www.ncbi.nlm.nih.gov/entrez/query.fcgi?cmd=Retrieve&db=PubMed&dopt=Citation&list_uids=20498018. doi:jcb.200910043 [pii] 10.1083/jcb.200910043
- Chakraborty, P., Seemann, J., Mishra, R. K., Wei, J. H., Weil, L., Nussenzveig, D. R., . . . Fontoura, B. M. (2009). Vesicular stomatitis virus inhibits mitotic progression and triggers cell death. *EMBO Rep*, *10*(10), 1154-1160. Retrieved from <https://www.ncbi.nlm.nih.gov/pubmed/19745842>. doi:10.1038/embor.2009.179
- Chakraborty, P., Wang, Y., Wei, J. H., van Deursen, J., Yu, H., Malureanu, L., . . . Fontoura, B. M. (2008). Nucleoporin levels regulate cell cycle progression and phase-specific gene expression. *Dev Cell*, *15*(5), 657-667. Retrieved from <https://www.ncbi.nlm.nih.gov/pubmed/19000832>. doi:10.1016/j.devcel.2008.08.020
- Chen, J., Smoyer, C. J., Slaughter, B. D., Unruh, J. R., & Jaspersen, S. L. (2014). The SUN protein Mps3 controls Ndc1 distribution and function on the nuclear

- membrane. *J Cell Biol*, 204(4), 523-539. Retrieved from <http://www.ncbi.nlm.nih.gov/pubmed/24515347>. doi:10.1083/jcb.201307043
- Ciska, M., & Moreno Diaz de la Espina, S. (2014). The intriguing plant nuclear lamina. *Front Plant Sci*, 5, 166. Retrieved from <http://www.ncbi.nlm.nih.gov/pubmed/24808902>. doi:10.3389/fpls.2014.00166
- Cristea, I. M., Williams, R., Chait, B. T., & Rout, M. P. (2005). Fluorescent proteins as proteomic probes. *Mol Cell Proteomics*, 4(12), 1933-1941. Retrieved from http://www.ncbi.nlm.nih.gov/entrez/query.fcgi?cmd=Retrieve&db=PubMed&dopt=Citation&list_uids=16155292.
- Cronshaw, J. M., Krutchinsky, A. N., Zhang, W., Chait, B. T., & Matunis, M. J. (2002). Proteomic analysis of the mammalian nuclear pore complex. *J Cell Biol*, 158(5), 915-927. Retrieved from http://www.ncbi.nlm.nih.gov/entrez/query.fcgi?cmd=Retrieve&db=PubMed&dopt=Citation&list_uids=12196509.
- Cuylen, S., & Haering, C. H. (2011). Deciphering condensin action during chromosome segregation. *Trends Cell Biol*, 21(9), 552-559. Retrieved from <https://www.ncbi.nlm.nih.gov/pubmed/21763138>. doi:10.1016/j.tcb.2011.06.003
- D'Angelo, M. A., Raices, M., Panowski, S. H., & Hetzer, M. W. (2009). Age-dependent deterioration of nuclear pore complexes causes a loss of nuclear integrity in postmitotic cells. *Cell*, 136(2), 284-295. Retrieved from http://www.ncbi.nlm.nih.gov/entrez/query.fcgi?cmd=Retrieve&db=PubMed&dopt=Citation&list_uids=19167330. doi:S0092-8674(08)01512-2 [pii] 10.1016/j.cell.2008.11.037
- Davidson, P. M., & Lammerding, J. (2014). Broken nuclei--lamins, nuclear mechanics, and disease. *Trends Cell Biol*, 24(4), 247-256. Retrieved from <https://www.ncbi.nlm.nih.gov/pubmed/24309562>. doi:10.1016/j.tcb.2013.11.004
- de Leeuw, R., Gruenbaum, Y., & Medalia, O. (2018). Nuclear Lamins: Thin Filaments with Major Functions. *Trends Cell Biol*, 28(1), 34-45. Retrieved from <https://www.ncbi.nlm.nih.gov/pubmed/28893461>. doi:10.1016/j.tcb.2017.08.004
- Dittmer, T. A., & Misteli, T. (2011). The lamin protein family. *Genome Biol*, 12(5), 222. Retrieved from <https://www.ncbi.nlm.nih.gov/pubmed/21639948>. doi:10.1186/gb-2011-12-5-222
- Doucet, C. M., & Hetzer, M. W. (2010). Nuclear pore biogenesis into an intact nuclear envelope. *Chromosoma*, 119(5), 469-477. Retrieved from http://www.ncbi.nlm.nih.gov/entrez/query.fcgi?cmd=Retrieve&db=PubMed&dopt=Citation&list_uids=20721671. doi:10.1007/s00412-010-0289-2
- Evans, L. M., Clark, J. S., Whipple, A. V., & Whitham, T. G. (2012). The relative influences of host plant genotype and yearly abiotic variability in determining herbivore abundance. *Oecologia*, 168(2), 483-489. Retrieved from <http://www.ncbi.nlm.nih.gov/pubmed/21918874>. doi:10.1007/s00442-011-2108-8
- Falini, B., Mecucci, C., Tiacci, E., Alcalay, M., Rosati, R., Pasqualucci, L., . . . Party, G. A. L. W. (2005). Cytoplasmic nucleophosmin in acute myelogenous leukemia with a normal karyotype. *N Engl J Med*, 352(3), 254-266. Retrieved from <https://www.ncbi.nlm.nih.gov/pubmed/15659725>. doi:10.1056/NEJMoa041974
- Faria, A. M., Levay, A., Wang, Y., Kamphorst, A. O., Rosa, M. L., Nussenzveig, D. R., . . . Fontoura, B. M. (2006). The nucleoporin Nup96 is required for proper

- expression of interferon-regulated proteins and functions. *Immunity*, 24(3), 295-304. Retrieved from <https://www.ncbi.nlm.nih.gov/pubmed/16546098>. doi:10.1016/j.immuni.2006.01.014
- Fernandez, P., Scaffidi, P., Markert, E., Lee, J. H., Rane, S., & Misteli, T. (2014). Transformation resistance in a premature aging disorder identifies a tumor-protective function of BRD4. *Cell Rep*, 9(1), 248-260. Retrieved from <https://www.ncbi.nlm.nih.gov/pubmed/25284786>. doi:10.1016/j.celrep.2014.08.069
- Finkbeiner, S. (2011). Huntington's Disease. *Cold Spring Harb Perspect Biol*, 3(6). Retrieved from <https://www.ncbi.nlm.nih.gov/pubmed/21441583>. doi:10.1101/cshperspect.a007476
- Floch, A. G., Palancade, B., & Doye, V. (2014). Fifty years of nuclear pores and nucleocytoplasmic transport studies: multiple tools revealing complex rules. *Methods Cell Biol*, 122, 1-40. Retrieved from <https://www.ncbi.nlm.nih.gov/pubmed/24857723>. doi:10.1016/B978-0-12-417160-2.00001-1
- Floch, A. G., Taresté, D., Fuchs, P. F., Chadrin, A., Naciri, I., Leger, T., . . . Doye, V. (2015). Nuclear pore targeting of the yeast Pom33 nucleoporin depends on karyopherin and lipid binding. *J Cell Sci*, 128(2), 305-316. Retrieved from <http://www.ncbi.nlm.nih.gov/pubmed/25413348>. doi:10.1242/jcs.158915
- Fontoura, B. M., Blobel, G., & Matunis, M. J. (1999). A conserved biogenesis pathway for nucleoporins: proteolytic processing of a 186-kilodalton precursor generates Nup98 and the novel nucleoporin, Nup96. *J Cell Biol*, 144(6), 1097-1112. Retrieved from http://www.ncbi.nlm.nih.gov/entrez/query.fcgi?cmd=Retrieve&db=PubMed&dopt=Citation&list_uids=10087256.
- Franks, T. M., McCloskey, A., Shokirev, M. N., Benner, C., Rathore, A., & Hetzer, M. W. (2017). Nup98 recruits the Wdr82-Set1A/COMPASS complex to promoters to regulate H3K4 trimethylation in hematopoietic progenitor cells. *Genes Dev*, 31(22), 2222-2234. Retrieved from <https://www.ncbi.nlm.nih.gov/pubmed/29269482>. doi:10.1101/gad.306753.117
- Franz, C., Askjaer, P., Antonin, W., Iglesias, C. L., Haselmann, U., Schelder, M., . . . Mattaj, I. W. (2005). Nup155 regulates nuclear envelope and nuclear pore complex formation in nematodes and vertebrates. *Embo J*, 24(20), 3519-3531. Retrieved from http://www.ncbi.nlm.nih.gov/entrez/query.fcgi?cmd=Retrieve&db=PubMed&dopt=Citation&list_uids=16193066. doi:7600825 [pii] 10.1038/sj.emboj.7600825
- Fujiwara, T., Tanaka, K., Kuroiwa, T., & Hirano, T. (2013). Spatiotemporal dynamics of condensins I and II: evolutionary insights from the primitive red alga *Cyanidioschyzon merolae*. *Mol Biol Cell*, 24(16), 2515-2527. Retrieved from <https://www.ncbi.nlm.nih.gov/pubmed/23783031>. doi:10.1091/mbc.E13-04-0208
- Funakoshi, T., Clever, M., Watanabe, A., & Imamoto, N. (2011). Localization of Pom121 to the inner nuclear membrane is required for an early step of interphase nuclear pore complex assembly. *Mol Biol Cell*, 22(7), 1058-1069. Retrieved from http://www.ncbi.nlm.nih.gov/entrez/query.fcgi?cmd=Retrieve&db=PubMed&dopt=Citation&list_uids=21511111.

t=Citation&list_uids=21289085. doi:mbc.E10-07-0641 [pii] 10.1091/mbc.E10-07-0641

- Funakoshi, T., Maeshima, K., Yahata, K., Sugano, S., Imamoto, F., & Imamoto, N. (2007). Two distinct human POM121 genes: requirement for the formation of nuclear pore complexes. *FEBS Lett*, *581*(25), 4910-4916. Retrieved from http://www.ncbi.nlm.nih.gov/entrez/query.fcgi?cmd=Retrieve&db=PubMed&dopt=Citation&list_uids=17900573. doi:S0014-5793(07)01003-4 [pii] 10.1016/j.febslet.2007.09.021
- Galy, V., Antonin, W., Jaedicke, A., Sachse, M., Santarella, R., Haselmann, U., & Mattaj, I. (2008). A role for gp210 in mitotic nuclear-envelope breakdown. *J Cell Sci*, *121*(Pt 3), 317-328. Retrieved from http://www.ncbi.nlm.nih.gov/entrez/query.fcgi?cmd=Retrieve&db=PubMed&dopt=Citation&list_uids=18216332. doi:121/3/317 [pii] 10.1242/jcs.022525
- Gerace, L., & Blobel, G. (1980). The nuclear envelope lamina is reversibly depolymerized during mitosis. *Cell*, *19*(1), 277-287. Retrieved from <https://www.ncbi.nlm.nih.gov/pubmed/7357605>.
- Gerhard-Herman, M., Smoot, L. B., Wake, N., Kieran, M. W., Kleinman, M. E., Miller, D. T., . . . Gordon, L. B. (2012). Mechanisms of premature vascular aging in children with Hutchinson-Gilford progeria syndrome. *Hypertension*, *59*(1), 92-97. Retrieved from <https://www.ncbi.nlm.nih.gov/pubmed/22083160>. doi:10.1161/HYPERTENSIONAHA.111.180919
- Gibbs, S. P. (1962a). Nuclear envelope-chloroplast relationships in algae. *J Cell Biol*, *14*, 433-444. Retrieved from <http://www.ncbi.nlm.nih.gov/pubmed/13947685>.
- Gibbs, S. P. (1962b). The ultrastructure of the chloroplasts of algae. *J Ultrastruct Res*, *7*, 418-435. Retrieved from <http://www.ncbi.nlm.nih.gov/pubmed/13947684>.
- Glavy, J. S., Krutchinsky, A. N., Cristea, I. M., Berke, I. C., Boehmer, T., Blobel, G., & Chait, B. T. (2007). Cell-cycle-dependent phosphorylation of the nuclear pore Nup107-160 subcomplex. *Proc Natl Acad Sci U S A*, *104*(10), 3811-3816. Retrieved from http://www.ncbi.nlm.nih.gov/entrez/query.fcgi?cmd=Retrieve&db=PubMed&dopt=Citation&list_uids=17360435. doi:0700058104 [pii] 10.1073/pnas.0700058104
- Gordon, L. B., Cao, K., & Collins, F. S. (2012). Progeria: translational insights from cell biology. *J Cell Biol*, *199*(1), 9-13. Retrieved from <http://www.ncbi.nlm.nih.gov/pubmed/23027899>. doi:10.1083/jcb.201207072
- Gordon, L. B., Kleinman, M. E., Miller, D. T., Neuberg, D. S., Giobbie-Hurder, A., Gerhard-Herman, M., . . . Kieran, M. W. (2012). Clinical trial of a farnesyltransferase inhibitor in children with Hutchinson-Gilford progeria syndrome. *Proc Natl Acad Sci U S A*, *109*(41), 16666-16671. Retrieved from <https://www.ncbi.nlm.nih.gov/pubmed/23012407>. doi:10.1073/pnas.1202529109
- Gordon, L. B., Rothman, F. G., Lopez-Otin, C., & Misteli, T. (2014). Progeria: a paradigm for translational medicine. *Cell*, *156*(3), 400-407. Retrieved from <https://www.ncbi.nlm.nih.gov/pubmed/24485450>. doi:10.1016/j.cell.2013.12.028
- Gordon, L. B., Shappell, H., Massaro, J., D'Agostino, R. B., Sr., Brazier, J., Campbell, S. E., . . . Kieran, M. W. (2018). Association of Lonafarnib Treatment vs No

- Treatment With Mortality Rate in Patients With Hutchinson-Gilford Progeria Syndrome. *JAMA*, 319(16), 1687-1695. Retrieved from <https://www.ncbi.nlm.nih.gov/pubmed/29710166>. doi:10.1001/jama.2018.3264
- Gough, S. M., Slape, C. I., & Aplan, P. D. (2011). NUP98 gene fusions and hematopoietic malignancies: common themes and new biologic insights. *Blood*, 118(24), 6247-6257. Retrieved from http://www.ncbi.nlm.nih.gov/entrez/query.fcgi?cmd=Retrieve&db=PubMed&dopt=Citation&list_uids=21948299. doi:10.1182/blood-2011-07-328880 [pii] 10.1182/blood-2011-07-328880
- Graumann, K., & Evans, D. E. (2011). Nuclear envelope dynamics during plant cell division suggest common mechanisms between kingdoms. *Biochem J*, 435(3), 661-667. Retrieved from <http://www.ncbi.nlm.nih.gov/pubmed/21323637>. doi:10.1042/BJ20101769
- Graziano, S., Kreienkamp, R., Coll-Bonfill, N., & Gonzalo, S. (2018). Causes and consequences of genomic instability in laminopathies: Replication stress and interferon response. *Nucleus*, 9(1), 258-275. Retrieved from <https://www.ncbi.nlm.nih.gov/pubmed/29637811>. doi:10.1080/19491034.2018.1454168
- Grima, J. C., Daigle, J. G., Arbez, N., Cunningham, K. C., Zhang, K., Ochaba, J., . . . Rothstein, J. D. (2017). Mutant Huntingtin Disrupts the Nuclear Pore Complex. *Neuron*, 94(1), 93-107 e106. Retrieved from <https://www.ncbi.nlm.nih.gov/pubmed/28384479>. doi:10.1016/j.neuron.2017.03.023
- Hashizume, C., Kobayashi, A., & Wong, R. W. (2013). Down-modulation of nucleoporin RanBP2/Nup358 impaired chromosomal alignment and induced mitotic catastrophe. *Cell Death Dis*, 4, e854. Retrieved from <https://www.ncbi.nlm.nih.gov/pubmed/24113188>. doi:10.1038/cddis.2013.370
- Hawryluk-Gara, L. A., Shibuya, E. K., & Wozniak, R. W. (2005). Vertebrate Nup53 interacts with the nuclear lamina and is required for the assembly of a Nup93-containing complex. *Mol Biol Cell*, 16(5), 2382-2394. Retrieved from http://www.ncbi.nlm.nih.gov/entrez/query.fcgi?cmd=Retrieve&db=PubMed&dopt=Citation&list_uids=15703211. doi:10.1091/mbc.E04-10-0857 [pii] 10.1091/mbc.E04-10-0857
- Hetzer, M. W., Walther, T. C., & Mattaj, I. W. (2005). Pushing the envelope: structure, function, and dynamics of the nuclear periphery. *Annu Rev Cell Dev Biol*, 21, 347-380. Retrieved from http://www.ncbi.nlm.nih.gov/entrez/query.fcgi?cmd=Retrieve&db=PubMed&dopt=Citation&list_uids=16212499. doi:10.1146/annurev.cellbio.21.090704.151152
- Hirano, T. (2012). Condensins: universal organizers of chromosomes with diverse functions. *Genes Dev*, 26(15), 1659-1678. Retrieved from <https://www.ncbi.nlm.nih.gov/pubmed/22855829>. doi:10.1101/gad.194746.112
- Hoelz, A., & Blobel, G. (2004). Cell biology: popping out of the nucleus. *Nature*, 432(7019), 815-816. Retrieved from http://www.ncbi.nlm.nih.gov/entrez/query.fcgi?cmd=Retrieve&db=PubMed&dopt=Citation&list_uids=15602540. doi:10.1038/432815a [pii] 10.1038/432815a

- Hoelz, A., Debler, E. W., & Blobel, G. (2011). The structure of the nuclear pore complex. *Annu Rev Biochem*, *80*, 613-643. Retrieved from <https://www.ncbi.nlm.nih.gov/pubmed/21495847>. doi:10.1146/annurev-biochem-060109-151030
- Hoelz, A., Glavy, J. S., & Beck, M. (2016). Toward the atomic structure of the nuclear pore complex: when top down meets bottom up. *Nat Struct Mol Biol*, *23*(7), 624-630. Retrieved from <https://www.ncbi.nlm.nih.gov/pubmed/27273515>. doi:10.1038/nsmb.3244
- Hogg, R. C., & Adams, D. J. (2001). An ATP-sensitive K(+) conductance in dissociated neurones from adult rat intracardiac ganglia. *J Physiol*, *534*(Pt 3), 713-720. Retrieved from <https://www.ncbi.nlm.nih.gov/pubmed/11483702>. doi:10.1111/j.1469-7793.2001.00713.x
- Imoto, Y., Fujiwara, T., Yoshida, Y., Kuroiwa, H., Maruyama, S., & Kuroiwa, T. (2010). Division of cell nuclei, mitochondria, plastids, and microbodies mediated by mitotic spindle poles in the primitive red alga *Cyanidioschyzon merolae*. *Protoplasma*, *241*(1-4), 63-74. Retrieved from <http://www.ncbi.nlm.nih.gov/pubmed/20148273>. doi:10.1007/s00709-010-0107-y
- Imoto, Y., Yoshida, Y., Yagisawa, F., Kuroiwa, H., & Kuroiwa, T. (2011). The cell cycle, including the mitotic cycle and organelle division cycles, as revealed by cytological observations. *J Electron Microsc (Tokyo)*, *60 Suppl 1*, S117-136. Retrieved from <http://www.ncbi.nlm.nih.gov/pubmed/21844584>. doi:10.1093/jmicro/df034
- Jaspersen, S. L., & Ghosh, S. (2012). Nuclear envelope insertion of spindle pole bodies and nuclear pore complexes. *Nucleus*, *3*(3), 226-236. Retrieved from http://www.ncbi.nlm.nih.gov/entrez/query.fcgi?cmd=Retrieve&db=PubMed&dopt=Citation&list_uids=22572959. doi:20148 [pii] 10.4161/nucl.20148
- Jeganathan, K. B., Malureanu, L., & van Deursen, J. M. (2005). The Rae1-Nup98 complex prevents aneuploidy by inhibiting securin degradation. *Nature*, *438*(7070), 1036-1039. Retrieved from http://www.ncbi.nlm.nih.gov/entrez/query.fcgi?cmd=Retrieve&db=PubMed&dopt=Citation&list_uids=16355229. doi:nature04221 [pii] 10.1038/nature04221
- Judy, S., & Schwartz, T. U. (2007). Crystal structure of nucleoporin Nic96 reveals a novel, intricate helical domain architecture. *J Biol Chem*, *282*(48), 34904-34912. Retrieved from http://www.ncbi.nlm.nih.gov/entrez/query.fcgi?cmd=Retrieve&db=PubMed&dopt=Citation&list_uids=17897938. doi:M705479200 [pii] 10.1074/jbc.M705479200
- Jeyasekharan, A. D., Liu, Y., Hattori, H., Pisupati, V., Jonsdottir, A. B., Rajendra, E., . . . Venkitaraman, A. R. (2013). A cancer-associated BRCA2 mutation reveals masked nuclear export signals controlling localization. *Nat Struct Mol Biol*, *20*(10), 1191-1198. Retrieved from <https://www.ncbi.nlm.nih.gov/pubmed/24013206>. doi:10.1038/nsmb.2666
- Kabachinski, G., & Schwartz, T. U. (2015). The nuclear pore complex--structure and function at a glance. *J Cell Sci*, *128*(3), 423-429. Retrieved from <https://www.ncbi.nlm.nih.gov/pubmed/26046137>.

- Kalverda, B., Pickersgill, H., Shloma, V. V., & Fornerod, M. (2010). Nucleoporins directly stimulate expression of developmental and cell-cycle genes inside the nucleoplasm. *Cell*, *140*(3), 360-371. Retrieved from <https://www.ncbi.nlm.nih.gov/pubmed/20144760>. doi:10.1016/j.cell.2010.01.011
- Knockenbauer, K. E., & Schwartz, T. U. (2016). The Nuclear Pore Complex as a Flexible and Dynamic Gate. *Cell*, *164*(6), 1162-1171. Retrieved from <https://www.ncbi.nlm.nih.gov/pubmed/26967283>. doi:10.1016/j.cell.2016.01.034
- Kosinski, J., Mosalaganti, S., von Appen, A., Teimer, R., DiGuilio, A. L., Wan, W., . . . Beck, M. (2016). Molecular architecture of the inner ring scaffold of the human nuclear pore complex. *Science*, *352*(6283), 363-365. Retrieved from <https://www.ncbi.nlm.nih.gov/pubmed/27081072>. doi:10.1126/science.aaf0643
- Kupke, T., Malsam, J., & Schiebel, E. (2017). A ternary membrane protein complex anchors the spindle pole body in the nuclear envelope in budding yeast. *J Biol Chem*, *292*(20), 8447-8458. Retrieved from <https://www.ncbi.nlm.nih.gov/pubmed/28356353>. doi:10.1074/jbc.M117.780601
- Laurell, E., Beck, K., Krupina, K., Theerthagiri, G., Bodenmiller, B., Horvath, P., . . . Kutay, U. (2011). Phosphorylation of Nup98 by multiple kinases is crucial for NPC disassembly during mitotic entry. *Cell*, *144*(4), 539-550. Retrieved from <https://www.ncbi.nlm.nih.gov/pubmed/21335236>. doi:10.1016/j.cell.2011.01.012
- Laurell, E., & Kutay, U. (2011). Dismantling the NPC permeability barrier at the onset of mitosis. *Cell Cycle*, *10*(14). Retrieved from http://www.ncbi.nlm.nih.gov/entrez/query.fcgi?cmd=Retrieve&db=PubMed&dopt=Citation&list_uids=21636979. doi:16195 [pii]
- Liang, Y., Franks, T. M., Marchetto, M. C., Gage, F. H., & Hetzer, M. W. (2013). Dynamic association of NUP98 with the human genome. *PLoS Genet*, *9*(2), e1003308. Retrieved from <http://www.ncbi.nlm.nih.gov/pubmed/23468646>. doi:10.1371/journal.pgen.1003308
- Lim, R. Y., Aebi, U., & Fahrenkrog, B. (2008). Towards reconciling structure and function in the nuclear pore complex. *Histochem Cell Biol*, *129*(2), 105-116. Retrieved from http://www.ncbi.nlm.nih.gov/entrez/query.fcgi?cmd=Retrieve&db=PubMed&dopt=Citation&list_uids=18228033. doi:10.1007/s00418-007-0371-x
- Linder, M. I., Kohler, M., Boersema, P., Weberruss, M., Wandke, C., Marino, J., . . . Kutay, U. (2017). Mitotic Disassembly of Nuclear Pore Complexes Involves CDK1- and PLK1-Mediated Phosphorylation of Key Interconnecting Nucleoporins. *Dev Cell*, *43*(2), 141-156 e147. Retrieved from <https://www.ncbi.nlm.nih.gov/pubmed/29065306>. doi:10.1016/j.devcel.2017.08.020
- Loiodice, I., Alves, A., Rabut, G., Van Overbeek, M., Ellenberg, J., Sibarita, J. B., & Doye, V. (2004). The entire Nup107-160 complex, including three new members, is targeted as one entity to kinetochores in mitosis. *Mol Biol Cell*, *15*(7), 3333-3344. Retrieved from http://www.ncbi.nlm.nih.gov/entrez/query.fcgi?cmd=Retrieve&db=PubMed&dopt=Citation&list_uids=15146057. doi:10.1091/mbc.E03-12-0878 E03-12-0878 [pii]

- Lusk, C. P., Blobel, G., & King, M. C. (2007). Highway to the inner nuclear membrane: rules for the road. *Nat Rev Mol Cell Biol*, 8(5), 414-420. Retrieved from <http://www.nature.com/nrm/journal/v8/n5/abs/nrm2165.html>
- Lutzmann, M., Kunze, R., Buerer, A., Aebi, U., & Hurt, E. (2002). Modular self-assembly of a Y-shaped multiprotein complex from seven nucleoporins. *Embo J*, 21(3), 387-397. Retrieved from http://www.ncbi.nlm.nih.gov/entrez/query.fcgi?cmd=Retrieve&db=PubMed&dopt=Citation&list_uids=11823431.
- Mansfeld, J., Guttinger, S., Hawryluk-Gara, L. A., Pante, N., Mall, M., Galy, V., . . . Antonin, W. (2006). The conserved transmembrane nucleoporin NDC1 is required for nuclear pore complex assembly in vertebrate cells. *Mol Cell*, 22(1), 93-103. Retrieved from http://www.ncbi.nlm.nih.gov/entrez/query.fcgi?cmd=Retrieve&db=PubMed&dopt=Citation&list_uids=16600873. doi:S1097-2765(06)00117-1 [pii] 10.1016/j.molcel.2006.02.015
- Matsuzaki, M., Misumi, O., Shin, I. T., Maruyama, S., Takahara, M., Miyagishima, S. Y., . . . Kuroiwa, T. (2004). Genome sequence of the ultrasmall unicellular red alga *Cyanidioschyzon merolae* 10D. *Nature*, 428(6983), 653-657. Retrieved from <http://www.ncbi.nlm.nih.gov/pubmed/15071595>. doi:10.1038/nature02398
- McClintock, D., Ratner, D., Lokuge, M., Owens, D. M., Gordon, L. B., Collins, F. S., & Djabali, K. (2007). The mutant form of lamin A that causes Hutchinson-Gilford progeria is a biomarker of cellular aging in human skin. *PLoS One*, 2(12), e1269. Retrieved from <https://www.ncbi.nlm.nih.gov/pubmed/18060063>. doi:10.1371/journal.pone.0001269
- Meier, I. (2001). The plant nuclear envelope. *Cell Mol Life Sci*, 58(12-13), 1774-1780. Retrieved from <http://www.ncbi.nlm.nih.gov/pubmed/11766878>.
- Melcak, I., Hoelz, A., & Blobel, G. (2007). Structure of Nup58/45 suggests flexible nuclear pore diameter by intermolecular sliding. *Science*, 315(5819), 1729-1732. Retrieved from http://www.ncbi.nlm.nih.gov/entrez/query.fcgi?cmd=Retrieve&db=PubMed&dopt=Citation&list_uids=17379812. doi:315/5819/1729 [pii] 10.1126/science.1135730
- Misumi, O., Matsuzaki, M., Nozaki, H., Miyagishima, S. Y., Mori, T., Nishida, K., . . . Kuroiwa, T. (2005). *Cyanidioschyzon merolae* genome. A tool for facilitating comparable studies on organelle biogenesis in photosynthetic eukaryotes. *Plant Physiol*, 137(2), 567-585. Retrieved from <https://www.ncbi.nlm.nih.gov/pubmed/15681662>. doi:10.1104/pp.104.053991
- Mitchell, J. M., Mansfeld, J., Capitano, J., Kutay, U., & Wozniak, R. W. (2010). Pom121 links two essential subcomplexes of the nuclear pore complex core to the membrane. *J Cell Biol*, 191(3), 505-521. Retrieved from http://www.ncbi.nlm.nih.gov/entrez/query.fcgi?cmd=Retrieve&db=PubMed&dopt=Citation&list_uids=20974814. doi:jcb.201007098 [pii] 10.1083/jcb.201007098

- Mor, A., White, M. A., & Fontoura, B. M. (2014). Nuclear trafficking in health and disease. *Curr Opin Cell Biol*, 28, 28-35. Retrieved from <https://www.ncbi.nlm.nih.gov/pubmed/24530809>. doi:10.1016/j.ceb.2014.01.007
- Mosalaganti, S., Kosinski, J., Albert, S., Schaffer, M., Strenkert, D., Salome, P. A., . . . Beck, M. (2018). In situ architecture of the algal nuclear pore complex. *Nat Commun*, 9(1), 2361. Retrieved from <https://www.ncbi.nlm.nih.gov/pubmed/29915221>. doi:10.1038/s41467-018-04739-y
- Napetschnig, J., Blobel, G., & Hoelz, A. (2007). Crystal structure of the N-terminal domain of the human protooncogene Nup214/CAN. *Proc Natl Acad Sci U S A*, 104(6), 1783-1788. Retrieved from http://www.ncbi.nlm.nih.gov/entrez/query.fcgi?cmd=Retrieve&db=PubMed&dopt=Citation&list_uids=17264208. doi:0610828104 [pii] 10.1073/pnas.0610828104
- Neumann, N., Jeffares, D. C., & Poole, A. M. (2006). Outsourcing the nucleus: nuclear pore complex genes are no longer encoded in nucleomorph genomes. *Evol Bioinform Online*, 2, 23-34. Retrieved from <http://www.ncbi.nlm.nih.gov/pubmed/19455199>.
- Ohnuma, M., Misumi, O., Fujiwara, T., Watanabe, S., Tanaka, K., & Kuroiwa, T. (2009). Transient gene suppression in a red alga, *Cyanidioschyzon merolae* 10D. *Protoplasma*, 236(1-4), 107-112. Retrieved from <https://www.ncbi.nlm.nih.gov/pubmed/19533298>. doi:10.1007/s00709-009-0056-5
- Ohnuma, M., Yokoyama, T., Inouye, T., Sekine, Y., & Tanaka, K. (2008). Polyethylene glycol (PEG)-mediated transient gene expression in a red alga, *Cyanidioschyzon merolae* 10D. *Plant Cell Physiol*, 49(1), 117-120. Retrieved from <https://www.ncbi.nlm.nih.gov/pubmed/18003671>. doi:10.1093/pcp/pcm157
- Olive, M., Harten, I., Mitchell, R., Beers, J. K., Djabali, K., Cao, K., . . . Gordon, L. B. (2010). Cardiovascular pathology in Hutchinson-Gilford progeria: correlation with the vascular pathology of aging. *Arterioscler Thromb Vasc Biol*, 30(11), 2301-2309. Retrieved from <https://www.ncbi.nlm.nih.gov/pubmed/20798379>. doi:10.1161/ATVBAHA.110.209460
- Onischenko, E., Stanton, L. H., Madrid, A. S., Kieselbach, T., & Weis, K. (2009). Role of the Ndc1 interaction network in yeast nuclear pore complex assembly and maintenance. *J Cell Biol*, 185(3), 475-491. Retrieved from http://www.ncbi.nlm.nih.gov/entrez/query.fcgi?cmd=Retrieve&db=PubMed&dopt=Citation&list_uids=19414609. doi:jcb.200810030 [pii] 10.1083/jcb.200810030
- Ori, A., Banterle, N., Iskar, M., Andres-Pons, A., Escher, C., Khanh Bui, H., . . . Beck, M. (2013). Cell type-specific nuclear pores: a case in point for context-dependent stoichiometry of molecular machines. *Mol Syst Biol*, 9, 648. Retrieved from <http://www.ncbi.nlm.nih.gov/pubmed/23511206>. doi:10.1038/msb.2013.4
- Park, N., Katikaneni, P., Skern, T., & Gustin, K. E. (2008). Differential targeting of nuclear pore complex proteins in poliovirus-infected cells. *J Virol*, 82(4), 1647-1655. Retrieved from <https://www.ncbi.nlm.nih.gov/pubmed/18045934>. doi:10.1128/JVI.01670-07

- Popovici, V., Budinska, E., Tejpar, S., Weinrich, S., Estrella, H., Hodgson, G., . . . Delorenzi, M. (2012). Identification of a poor-prognosis BRAF-mutant-like population of patients with colon cancer. *J Clin Oncol*, *30*(12), 1288-1295. Retrieved from <https://www.ncbi.nlm.nih.gov/pubmed/22393095>. doi:10.1200/JCO.2011.39.5814
- Rajanala, K., & Nandicoori, V. K. (2012). Localization of nucleoporin Tpr to the nuclear pore complex is essential for Tpr mediated regulation of the export of unspliced RNA. *PLoS One*, *7*(1), e29921. Retrieved from <https://www.ncbi.nlm.nih.gov/pubmed/22253824>. doi:10.1371/journal.pone.0029921
- Rajanala, K., Sarkar, A., Jhingan, G. D., Priyadarshini, R., Jalan, M., Sengupta, S., & Nandicoori, V. K. (2014). Phosphorylation of nucleoporin Tpr governs its differential localization and is required for its mitotic function. *J Cell Sci*, *127*(Pt 16), 3505-3520. Retrieved from <https://www.ncbi.nlm.nih.gov/pubmed/24938596>. doi:10.1242/jcs.149112
- Rosenblum, J. S., & Blobel, G. (1999). Autoproteolysis in nucleoporin biogenesis. *Proc Natl Acad Sci U S A*, *96*(20), 11370-11375. Retrieved from http://www.ncbi.nlm.nih.gov/entrez/query.fcgi?cmd=Retrieve&db=PubMed&dopt=Citation&list_uids=10500183.
- Rout, M. P., Aitchison, J. D., Suprpto, A., Hjertaas, K., Zhao, Y., & Chait, B. T. (2000). The yeast nuclear pore complex: composition, architecture, and transport mechanism. *J Cell Biol*, *148*(4), 635-651. Retrieved from http://www.ncbi.nlm.nih.gov/entrez/query.fcgi?cmd=Retrieve&db=PubMed&dopt=Citation&list_uids=10684247.
- Rout, M. P., & Wente, S. R. (1994). Pores for thought: nuclear pore complex proteins. *Trends Cell Biol*, *4*(10), 357-365. Retrieved from http://www.ncbi.nlm.nih.gov/entrez/query.fcgi?cmd=Retrieve&db=PubMed&dopt=Citation&list_uids=14731624. doi:096289249490085X [pii]
- Sakuma, S., & D'Angelo, M. A. (2017). The roles of the nuclear pore complex in cellular dysfunction, aging and disease. *Semin Cell Dev Biol*, *68*, 72-84. Retrieved from <https://www.ncbi.nlm.nih.gov/pubmed/28506892>. doi:10.1016/j.semcdb.2017.05.006
- Samudio, I., Konopleva, M., Hail, N., Jr., Shi, Y. X., McQueen, T., Hsu, T., . . . Andreeff, M. (2005). 2-Cyano-3,12-dioxooleana-1,9-dien-28-imidazolide (CDDO-Im) directly targets mitochondrial glutathione to induce apoptosis in pancreatic cancer. *J Biol Chem*, *280*(43), 36273-36282. Retrieved from <https://www.ncbi.nlm.nih.gov/pubmed/16118208>. doi:10.1074/jbc.M507518200
- Satterly, N., Tsai, P. L., van Deursen, J., Nussenzveig, D. R., Wang, Y., Faria, P. A., . . . Fontoura, B. M. (2007). Influenza virus targets the mRNA export machinery and the nuclear pore complex. *Proc Natl Acad Sci U S A*, *104*(6), 1853-1858. Retrieved from <https://www.ncbi.nlm.nih.gov/pubmed/17267598>. doi:10.1073/pnas.0610977104
- Savas, J. N., Toyama, B. H., Xu, T., Yates, J. R., 3rd, & Hetzer, M. W. (2012). Extremely long-lived nuclear pore proteins in the rat brain. *Science*, *335*(6071), 942. Retrieved from <https://www.ncbi.nlm.nih.gov/pubmed/22300851>. doi:10.1126/science.1217421

- Schaffer, M., Engel, B. D., Laugks, T., Mahamid, J., Plitzko, J. M., & Baumeister, W. (2015). Cryo-focused Ion Beam Sample Preparation for Imaging Vitreous Cells by Cryo-electron Tomography. *Bio Protoc*, 5(17). Retrieved from <https://www.ncbi.nlm.nih.gov/pubmed/27294174>.
- Schwartz, T. U. (2005). Modularity within the architecture of the nuclear pore complex. *Curr Opin Struct Biol*, 15(2), 221-226. Retrieved from http://www.ncbi.nlm.nih.gov/entrez/query.fcgi?cmd=Retrieve&db=PubMed&dopt=Citation&list_uids=15837182.
- Shaulov, L., Gruber, R., Cohen, I., & Harel, A. (2011). A dominant-negative form of POM121 binds chromatin and disrupts the two separate modes of nuclear pore assembly. *J Cell Sci*, 124(Pt 22), 3822-3834. Retrieved from http://www.ncbi.nlm.nih.gov/entrez/query.fcgi?cmd=Retrieve&db=PubMed&dopt=Citation&list_uids=22100917. doi:jcs.086660 [pii] 10.1242/jcs.086660
- Sikorskaite, S., Rajamaki, M. L., Baniulis, D., Stanys, V., & Valkonen, J. P. (2013). Protocol: Optimised methodology for isolation of nuclei from leaves of species in the Solanaceae and Rosaceae families. *Plant Methods*, 9, 31. Retrieved from <https://www.ncbi.nlm.nih.gov/pubmed/23886449>. doi:10.1186/1746-4811-9-31
- Stavru, F., Hulsmann, B. B., Spang, A., Hartmann, E., Cordes, V. C., & Gorlich, D. (2006). NDC1: a crucial membrane-integral nucleoporin of metazoan nuclear pore complexes. *J Cell Biol*, 173(4), 509-519. Retrieved from http://www.ncbi.nlm.nih.gov/entrez/query.fcgi?cmd=Retrieve&db=PubMed&dopt=Citation&list_uids=16702233. doi:jcb.200601001 [pii] 10.1083/jcb.200601001
- Stuwe, T., Correia, A. R., Lin, D. H., Paduch, M., Lu, V. T., Kossiakoff, A. A., & Hoelz, A. (2015). Nuclear pores. Architecture of the nuclear pore complex coat. *Science*, 347(6226), 1148-1152. Retrieved from <https://www.ncbi.nlm.nih.gov/pubmed/25745173>. doi:10.1126/science.aaa4136
- Takeda, A., Goolsby, C., & Yaseen, N. R. (2006). NUP98-HOXA9 induces long-term proliferation and blocks differentiation of primary human CD34+ hematopoietic cells. *Cancer Res*, 66(13), 6628-6637. Retrieved from <https://www.ncbi.nlm.nih.gov/pubmed/16818636>. doi:10.1158/0008-5472.CAN-06-0458
- Tamura, K., Fukao, Y., Iwamoto, M., Haraguchi, T., & Hara-Nishimura, I. (2010). Identification and characterization of nuclear pore complex components in *Arabidopsis thaliana*. *Plant Cell*, 22(12), 4084-4097. Retrieved from <http://www.ncbi.nlm.nih.gov/pubmed/21189294>. doi:10.1105/tpc.110.079947
- Tang, Y., Chen, Y., Jiang, H., & Nie, D. (2010). Promotion of tumor development in prostate cancer by progerin. *Cancer Cell Int*, 10, 47. Retrieved from <https://www.ncbi.nlm.nih.gov/pubmed/21106101>. doi:10.1186/1475-2867-10-47
- Toyama, B. H., Savas, J. N., Park, S. K., Harris, M. S., Ingolia, N. T., Yates, J. R., 3rd, & Hetzer, M. W. (2013). Identification of long-lived proteins reveals exceptional stability of essential cellular structures. *Cell*, 154(5), 971-982. Retrieved from <https://www.ncbi.nlm.nih.gov/pubmed/23993091>. doi:10.1016/j.cell.2013.07.037
- Tran, E. J., & Wenthe, S. R. (2006). Dynamic nuclear pore complexes: life on the edge. *Cell*, 125(6), 1041-1053. Retrieved from

- http://www.ncbi.nlm.nih.gov/entrez/query.fcgi?cmd=Retrieve&db=PubMed&dopt=Citation&list_uids=16777596.
- Vecchione, L., Gambino, V., Raaijmakers, J., Schlicker, A., Fumagalli, A., Russo, M., . . . Bernards, R. (2016). A Vulnerability of a Subset of Colon Cancers with Potential Clinical Utility. *Cell*, *165*(2), 317-330. Retrieved from <https://www.ncbi.nlm.nih.gov/pubmed/27058664>. doi:10.1016/j.cell.2016.02.059
- von Appen, A., Kosinski, J., Sparks, L., Ori, A., DiGuilio, A. L., Vollmer, B., . . . Beck, M. (2015). In situ structural analysis of the human nuclear pore complex. *Nature*, *526*(7571), 140-143. Retrieved from <https://www.ncbi.nlm.nih.gov/pubmed/26416747>. doi:10.1038/nature15381
- Walther, T. C., Alves, A., Pickersgill, H., Liodice, I., Hetzer, M., Galy, V., . . . Doye, V. (2003). The conserved Nup107-160 complex is critical for nuclear pore complex assembly. *Cell*, *113*(2), 195-206. Retrieved from http://www.ncbi.nlm.nih.gov/entrez/query.fcgi?cmd=Retrieve&db=PubMed&dopt=Citation&list_uids=12705868.
- Watanabe, S., Ohnuma, M., Sato, J., Yoshikawa, H., & Tanaka, K. (2011). Utility of a GFP reporter system in the red alga *Cyanidioschyzon merolae*. *J Gen Appl Microbiol*, *57*(1), 69-72. Retrieved from <https://www.ncbi.nlm.nih.gov/pubmed/21478650>.
- Webster, M., Witkin, K. L., & Cohen-Fix, O. (2009). Sizing up the nucleus: nuclear shape, size and nuclear-envelope assembly. *J Cell Sci*, *122*(Pt 10), 1477-1486. Retrieved from <http://www.ncbi.nlm.nih.gov/pubmed/19420234>. doi:10.1242/jcs.037333
- Weis, K. (2003). Regulating access to the genome: nucleocytoplasmic transport throughout the cell cycle. *Cell*, *112*(4), 441-451. Retrieved from http://www.ncbi.nlm.nih.gov/entrez/query.fcgi?cmd=Retrieve&db=PubMed&dopt=Citation&list_uids=12600309. doi:S0092867403000825 [pii]
- Wong, R. W., & D'Angelo, M. (2016). Linking Nucleoporins, Mitosis, and Colon Cancer. *Cell Chem Biol*, *23*(5), 537-539. Retrieved from <https://www.ncbi.nlm.nih.gov/pubmed/27203373>. doi:10.1016/j.chembiol.2016.05.004
- Worman, H. J., & Bonne, G. (2007). "Laminopathies": a wide spectrum of human diseases. *Exp Cell Res*, *313*(10), 2121-2133. Retrieved from <https://www.ncbi.nlm.nih.gov/pubmed/17467691>. doi:10.1016/j.yexcr.2007.03.028
- Yagisawa, F., Fujiwara, T., Kuroiwa, H., Nishida, K., Imoto, Y., & Kuroiwa, T. (2012). Mitotic inheritance of endoplasmic reticulum in the primitive red alga *Cyanidioschyzon merolae*. *Protoplasma*, *249*(4), 1129-1135. Retrieved from <https://www.ncbi.nlm.nih.gov/pubmed/22160190>. doi:10.1007/s00709-011-0359-1
- Yagisawa, F., Fujiwara, T., Ohnuma, M., Kuroiwa, H., Nishida, K., Imoto, Y., . . . Kuroiwa, T. (2013). Golgi inheritance in the primitive red alga, *Cyanidioschyzon merolae*. *Protoplasma*, *250*(4), 943-948. Retrieved from <https://www.ncbi.nlm.nih.gov/pubmed/23197134>. doi:10.1007/s00709-012-0467-6

- Zhang, D., & Oliferenko, S. (2013). Remodeling the nuclear membrane during closed mitosis. *Curr Opin Cell Biol*, 25(1), 142-148. Retrieved from <http://www.ncbi.nlm.nih.gov/pubmed/23040820>. doi:10.1016/j.ceb.2012.09.001
- Zhang, K., Donnelly, C. J., Haeusler, A. R., Grima, J. C., Machamer, J. B., Steinwald, P., . . . Rothstein, J. D. (2015). The C9orf72 repeat expansion disrupts nucleocytoplasmic transport. *Nature*, 525(7567), 56-61. Retrieved from <https://www.ncbi.nlm.nih.gov/pubmed/26308891>. doi:10.1038/nature14973

Appendix A: Preparation of Nuclear Extract Solutions

Solution A (RSB, in DI water)

- 10 mM Tris, pH 7.4
- 10 mM NaCl (Fisher, 7647-14-5)
- 3 mM MgCl₂
- Protease inhibitors (Sigma-Aldrich Protease Inhibitor Cocktail, P2714-1BTL) may be added to a final 100 U/mL concentration

Solution B (RSBG 40, in DI water)

- 10 mM Tris, pH 7.4 (Tris HCl may be used)
- 10 mM NaCl
- 3 mM MgCl₂
- 10% Glycerol
- 0.5% Nonidet P40 (US Biological Life Sciences, L15081874)
- 0.5 mM DTT
- 100 U/mL protease inhibitors (for protein studies)
- 100 U/mL RNase A (Sigma-Aldrich, R4642)
- 100 U/mL DNase I (Sigma-Aldrich, D-5307)

Detergent Solution (in DI water)

- 3.3% wt/wt solution Sodium Deoxycholate
- 6.6% vol/vol Tween 40

Appendix B: Preparation of Complete Buffer Solution for Chloroplast Isolation

- 2X Chloroplast Isolation Buffer Stock – dilute 1:1 with dH₂O
- 10% BSA solution – 10 μ L added per 1 mL of 1X Chloroplast Isolation Buffer
- DTT – 1 μ L added per 1 mL of Chloroplast Isolation Buffer
- Protease inhibitors – 1 μ L added to final solution

Appendix C: Reagents used in Optimized Nuclei Isolation

Components of Storage Buffer:

Stock Concentration	Reagent	Storage Buffer (100mL)
2.66 M	Sucrose	9.4 mL
1M	50mM Tris (pH 7.5)	5 mL
1M	25mM KCl	2.5 mL
1M	5mM MgCl ₂	500 μ L
1M	2mM DTT	200 μ L
100X	Protease Inhibitor (1X)	1 mL
n/a	Millipore Water	81.4 mL